Single-Event Effects Testing with a Laser Beam - Guidelines

Vincent Pouget

Single-Event Effects Testing with a Laser Beam

-

Guidelines

Document information:

- reference: ESA-TN2
- contract No: 4000133635/20/NL/KML/rk
- version: 2 (final) - date:19/05/2022
- author: V. Pouget, IES, CNRS (vincent.pouget@umontpellier.fr)

IES | Institut d'Électronique et des Systèmes
UMR 5214 - CNRS - UM
Université de Montpellier

Campus St Priest
860 rue St Priest
Bâtiment 5 - CC 05001
34095 Montpellier CEDEX 5

tel +33 (0)4 67 14 37 16
fax +33 (0)4 67 54 71 34
www.ies.univ-montp2.fr

Revision history:

Date	Version	Revision
28/05/2021	0	Outline draft for review and discussion
01/12/2021	TN1	Draft for review
19/05/2022	TN2	Final deliverable version. Taking into consideration the comments, suggestions and corrections from: - Florent Miller - Dale McMorrow - Guillaume Bascoul - Alessandra Costantino - Thomas Borel - Christian Poivey

Contents

List of abbreviations

BGA	Ball grid array
CMOS	Complementary metal-oxide-semiconductor
DSM	Deep sub-micron
DUT	Device under test
FWHM	Full width at half maximum
LET	Linear energy transfer
MBU	Multiple bit upset
MCU	Multiple cell upset
NA	Numerical aperture
PCB	Printed circuit board
ROI	Region of interest
SEB	Single-event burn-out
SEE	Single-event effect
SEFI	Single-event functional interrupt
SEGR	Single-event gate rupture
SEL	Single-event latch-up
SET	Single-event transient
SEU	Single-event upset
SI	Système international
SOI	Silicon on insulator
SPA	Single-photon absorption
TPA	Two-photon absorption

1. Scope of the document

This document presents guidelines for testing single-event effects (SEE) in electronic components with a laser beam.

The SEE laser testing technique is a complement to the classical particle-beam-based techniques that can provide useful information on the sensitivity of a device to SEE. Since the first concept of the technique in the late eighties, the technique has been developed and its usage as a complementary tool has progressively spread in the last decades to cover many case studies. This development is motivated not only by the spatial and temporal resolutions of the technique but also by the availability and flexibility of an in-lab technique free from radiation safety constraints.

Due to the fundamental differences between the interaction of a particle and a laser pulse with a device, the experimental parameters and the method of the laser testing technique must be carefully defined in order to produce useful results in the context of radiation effects. In an effort to harmonize the way the technique is implemented and used, this document aims at summarizing the best practices in the field of SEE laser testing in order to facilitate the use of the technique by new users and to enable laser testing results comparison, exploitation, as well as their correlation with particle-beam results.

1.1. Principles of the guidelines

The goal of this document is to provide practical guidelines in order to facilitate the routine use of the laser testing technique by non-experts in an application-oriented context. Research-oriented uses of the laser testing technique, by their exploratory nature, may notably depart from those guidelines.

This document is not an help to decide whether the use of laser testing is appropriate for a project or not, because such decision involves project-level parameters and considerations that are out of the scope of this document. Instead, this document focuses on how laser testing should be performed to produce useful and reusable results.

This document focuses on the common base of the laser testing technique and does not include all possible facility-specific variations. It is the intent of this document to be as much facility-agnostic as possible, although some parameters and implementation recommendations are given when available in the common base.

This document is not an exhaustive review of the scientific literature on laser testing. It only provides a limited set of useful references.

This document targets engineers in electronics as a priority. The technical content on the physical optics side is voluntarily simplified to make it accessible to non-experts.

1.2. Silicon vs other materials

This document focuses on laser testing of silicon technologies. Many guidelines in this document may also be applicable to other technologies, but all numbers are specific to the test of silicon devices.

Laser testing of technologies based on other semiconductor materials is an active field of research, with references available in the literature, but its use is not sufficiently widely spread to define common values for important optical parameters.

2. Prerequisites & useful references

This document requires some basic knowledge of radiation-induced SEEs and the standard test methods used to evaluate those effects [1,2].

This document makes use of the standard acronyms for the various SEEs defined in [1,2].

3. Principles of SEE laser testing techniques

Laser testing for SEEs consists in using the photoelectric interaction of a short and focused laser pulse with the semiconductor material of a device to mimic the transient and localized track of electron-hole pairs produced by ionizing particles.

3.1. Fundamentals

This section introduces the fundamental concepts and definitions required for a good understanding of the laser testing technique and to perform any elementary modeling or calculation associated with laser testing. The reader more interested in practical considerations may jump directly to section 3.2.

The text and equations can include shortcuts in an attempt to make the involved optics and physics accessible to non-specialists. More details can be found in the indicated references.

All equations use the International System of Units (SI).

In all equations, the letter 'e' stands for Euler's number (exponential function).

3.1.1. Laser beam propagation

3.1.1.1. Gaussian beam definition

The envelope of the transverse electromagnetic wave of laser beams delivered by most commercial free-space lasers or single-mode fibers is well described by the fundamental Gauss-Hermite mode that constitutes an approximate solution of the Helmoltz equation of propagation within the paraxial (i.e. weak focusing) approximation [3]. This mode defines the so-called Gaussian beam, which is characterized by a Gaussian radial distribution of the field amplitude, and thus, of the optical intensity. As schematically presented in Fig. 3.1, the radial profile of the intensity gets sharper, i.e. with smaller width and higher amplitude, close to the beam-waist.

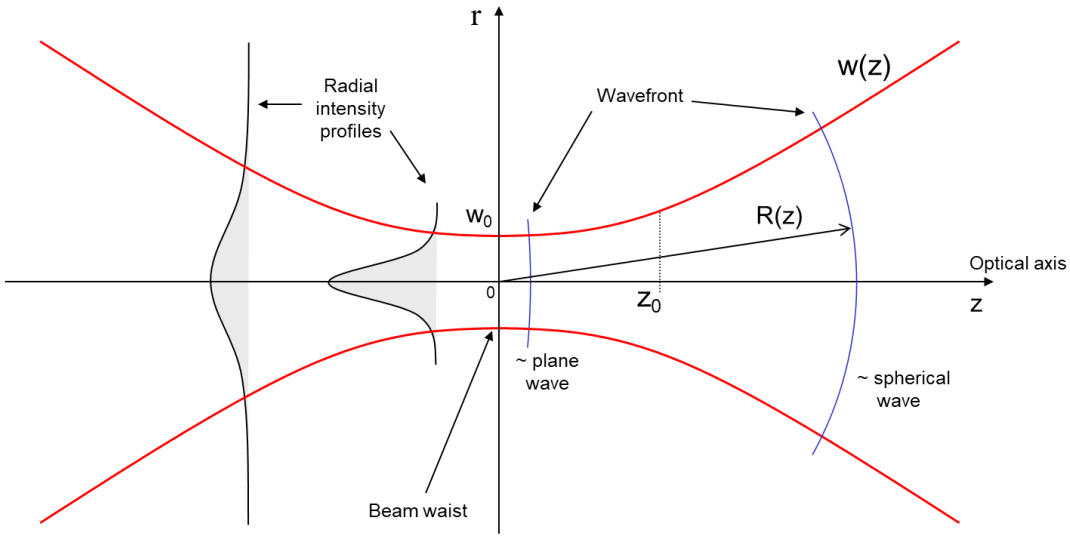

Fig. 3.1: schematic definition of a Gaussian laser beam

The optical intensity (or irradiance) of a pulsed Gaussian beam in vacuum (and within a good approximation, in air) is given by:

$$\mathrm{I}(r,z,t) = I_0 \frac{w_0^2}{w(z)^2} e^{-\frac{2r^2}{w(z)^2}} e^{-\frac{t^2}{\tau^2}} \quad (3\text{-}1)$$

Where I_0 is the peak intensity, τ is the pulse duration, and *w(z)* describes the evolution of the width of the radial profile along the optical axis, given by:

$$w(z) = w_0 \sqrt{1 + \left(\frac{z}{z_0}\right)^2} \quad (3\text{-}2)$$

where w_0 is the characteristic half width of the Gaussian radial profile at the beam-waist position, also shortly referred to as the beam-waist size, or simply the beam-waist. z_0 is the confocal or Rayleigh parameter of the beam given by:

$$z_0 = \frac{\pi w_0^2}{\lambda_0} \quad (3\text{-}3)$$

where λ_0 is the wavelength in vacuum. z_0 is the distance from the beam-waist position over which the beam-waist size increases by a factor $\sqrt{2}$. The shorter z_0 is, the faster the beam converge and diverge.

In (3-1), the time envelope has been simplified to a Gaussian pulse of duration τ by neglecting the pulse propagation, i.e. by considering that light propagation is instantaneous. In Silicon, the speed of light is around 100µm/ps, so this approximation is reasonable for the vast majority of semiconductor devices and should only be revisited for very thick sensitive volumes (>100µm) and very high-speed (>1THz) devices.

The peak intensity I_0 is related to the pulse energy E_0 by:

$$I_0 = \frac{2E_0}{\pi^{3/2} w_0^2 \tau} \quad (3\text{-}4)$$

Although not a commonly used quantity, the number of photons is given by:

$$N_\gamma = \frac{E_0}{E_\gamma} \quad (3\text{-}5)$$

where $E_\gamma = \hbar\omega$ is the photon energy related to the wavelength by:

$$E_\gamma = \frac{hc}{\lambda_0} \quad (3\text{-}6)$$

where *h* is the Planck constant, and *c* the speed of light in vacuum.

The radius of curvature of the electromagnetic wavefront of the Gaussian beam is given by:

$$R(z) = z\left(1 + \left(\frac{z_0}{z}\right)^2\right) \quad (3\text{-}7)$$

The wavefront can be assimilated to a plane wave near the beam-waist, while it tends to become spherical away from the focal region.

Another important parameter of a Gaussian beam is its divergence, defined as the asymptotic angle formed by w(z) with the optical axis:

$$\theta \approx \frac{\lambda_0}{\pi w_0} = \frac{w_0}{z_0} \quad (3\text{-}8)$$

The divergence of a beam is inversely proportional to the beam-waist size. Conversely, the beam-waist size will be inversely proportional to the converging angle that can be imposed by a focusing lens.

Due to the finite dimensions and other imperfections of optical elements, real laser beams can be more accurately described by a weighted sum of the fundamental Gaussian mode with higher order modes. This combination can be expressed by introducing a beam quality factor, noted M^2, which depends on the number and weights of the higher order modes that compose the beam [4]. The real beam is then described by substituting $z0$ by $z0/M^2$ in the previous equations and the divergence becomes:

$$\theta \approx M^2 \frac{\lambda_0}{\pi w_0} \tag{3-9}$$

An M^2 of 1 corresponds to a perfect Gaussian beam. Typical good quality laser sources deliver beams with M^2 between 1.1 than 1.3, but the M^2 of some sources, like laser diodes, multiple stage optical amplifiers or multimode fibers, can reach much higher values. Any diffracting element on the beam path will tend to increase the M^2 of the beam. The M^2 of a beam can be characterized experimentally from (3-9) by measuring the spot size and the far-field divergence.

3.1.1.2. Refraction

The equations above, defined in vacuum, can be transposed to the case of a Gaussian beam in a medium A of real refractive index n_A by replacing the wavelength in vacuum by the wavelength in the medium:

$$\lambda_A = \frac{\lambda_0}{n_A} \tag{3-10}$$

We can define the Rayleigh parameter in the medium by:

$$z_A = n_A z_0 \tag{3-11}$$

In the medium A, the beam-waist size, the wavefront radius of curvature evolution along the optical axis and the beam divergence are obtained by substituting z_0 with z_A in equations (3-2), (3-7) and (3-8), respectively. The effect of refraction on the propagation of a Gaussian beam can be easily conceptualized as a dilatation of the optical axis by a factor equal to the refractive index, as can be seen on fig. 3.2 which represents the case of

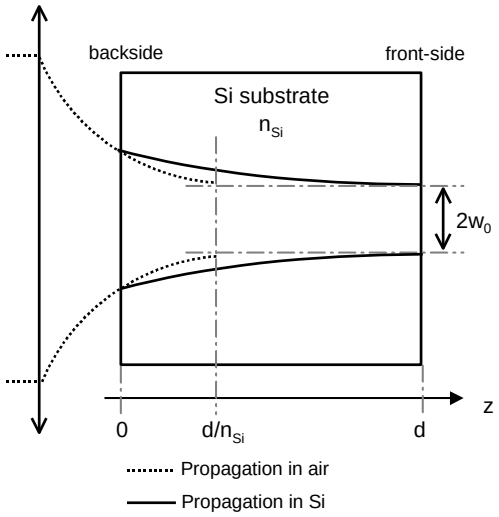

Fig. 3.2: effect of the refraction index on beam focusing through the substrate

focusing a beam through the backside of a silicon substrate. At the wavelength of 1064nm, the index of refraction of silicon is well approximated by $n_{Si} \approx 3.55$.

3.1.1.3. Reflection and Transmission at interfaces

Interfaces between different optical media, characterized by different refraction indexes or different absorption coefficients, partially reflect light. Considering an incident intensity I_0, the intensity transmitted through an interface is given by:

$$I_t = (1 - \mathrm{R})I_0 = \mathrm{T}\, I_0 \tag{3-12}$$

where R and T are the interface reflectance and transmittance coefficients, respectively. Those coefficients are easily calculated in the plane wave approximation using the Fresnel equations [5]. Table 3.1 gives estimations of the transmittance at 1064nm of some interfaces and stack of interest for SEE laser testing.

Table 3.1: Transmittance of common interfaces

Interface or stack	**Transmittance @ 1064nm @ normal incidence**
Air / Si	69 %
Si / SiO2	82 %
SiO_2 / Cu	4 %
SiO_2 / Al	6 %
SiO_2 / Cu (200nm) / SiO_2	< 10^{-5} %

3.1.2. Absorption mechanisms in semiconductors

3.1.2.1. Linear absorption

3.1.2.1.1. Band-to-band absorption

A photon with an energy higher than the band-gap of a semiconductor can be absorbed by an electron in the valence band. This absorption promotes the electron to the conduction band, creating an electron-hole pair. This

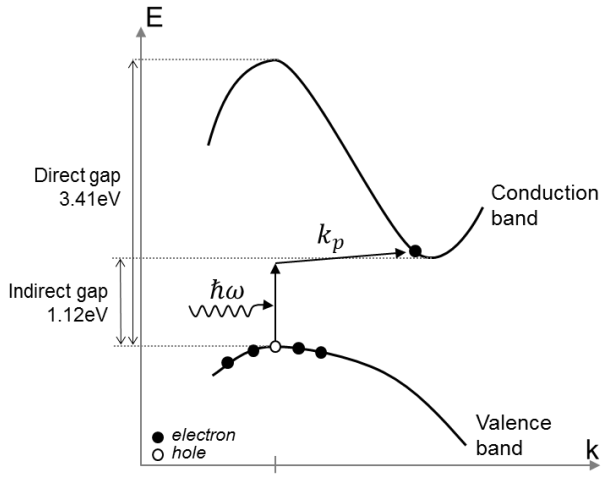

Fig. 3.3: simplified band diagram of silicon and principle of phonon-assisted indirect band-to-band absorption of a photon by an electron

absorption mechanism, known as the band-to-band (or interband) absorption, is responsible for the well-known photoelectric effect. In pure silicon, this absorption can occur for photons with an energy higher than the indirect band-gap (Eg=1.124eV at 300K). As presented in Fig. 3.3, this mechanism also involves the absorption of a phonon for impulse conservation and is thus sensitive to the lattice temperature [6-8].

The condition on the photon energy for interband absorption is:

$$E_\gamma > E_g \tag{3-13}$$

and can be expressed, in terms of wavelength, as:

$$\lambda_0 < \lambda_g \tag{3-14}$$

where λg is the band-gap wavelength and equals 1103nm at 300K in silicon. Photons with wavelength shorter than this value, situated in the near-infrared region of the optical spectrum, can be absorbed and produce electron-hole pairs in silicon.

3.1.2.1.2. Free-carrier absorption

Considering an electron in the conduction band, it can absorb a photon, without any condition on the photon energy, to reach a state of higher energy in the continuum of authorized energy states in the conduction band. This mechanism is known as the intraband or free-carrier absorption. This absorption does not create an electron-hole pair but simply increases the free carrier kinetic energy. Most of this excess of energy will then be transferred to the lattice as the carrier relaxes to the bottom of the conduction band through phonon interactions.

3.1.2.1.1. Optical absorption coefficient

Due to the different absorption mechanisms described above, a flux of photons gets attenuated as it propagates through the silicon. The probability of absorption at a given point in space is proportional to the photon density at that point [9]. The relative variation of the photon flux through an infinitesimal slab of material is then proportional to the slab thickness. Considering a monochromatic plane wave with an initial intensity I_0 propagating into a semiconductor, the intensity will decrease exponentially along the depth z into the material according to the macroscopic Beer-Lambert law:

$$\mathrm{I}(z) = I_0 e^{-\alpha \mathrm{z}} \tag{3-15}$$

where α is defined as the optical absorption coefficient.

The optical absorption coefficient in silicon, in the range of wavelengths of interest for SEE laser testing is the sum of two contributions:

$$\alpha = \alpha_{IB} + \alpha_{FC} \tag{3-16}$$

where α_{IB} is the interband absorption coefficient, i.e. the photoelectric contribution that generates electron-hole pairs, and α_{FC} is the free-carrier absorption coefficient, i.e. the photothermal contribution that does not contribute to electron-hole generation. The free-carrier contribution is highly dependent on the doping level and both terms are dependent on temperature. Fig 3.4 presents the absorption coefficient of silicon as a function of the photon energy for different doping levels [10].

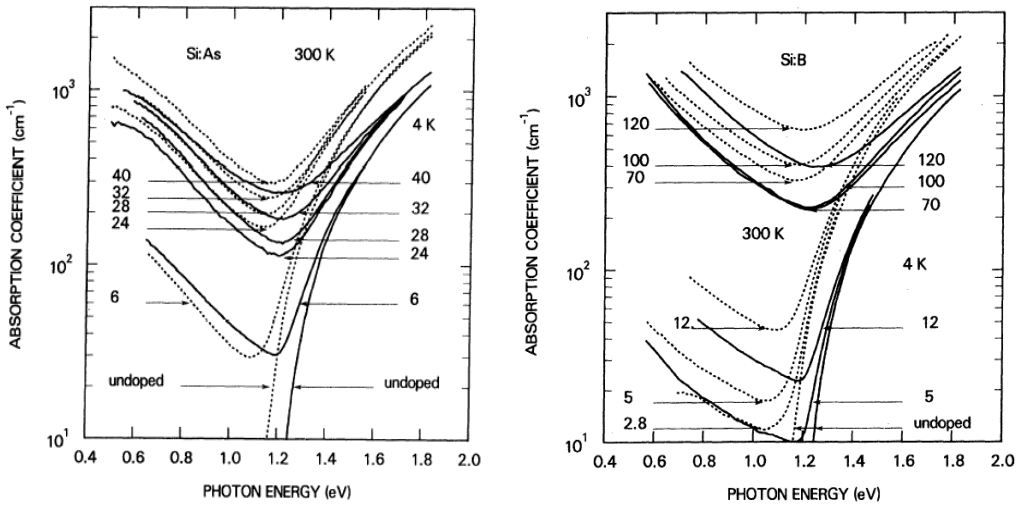

Fig. 3.4: absorption coefficient of N-doped (right) and P-doped (left) Silicon, from [10]

The *penetration depth* is defined as the depth at which the flux of photon is reduced by a factor $1/e$ and is given by:

$$d = \frac{1}{\alpha} \tag{3-17}$$

From the semiconductor material point of view, interband photon absorption will translate into an electron-hole pair generation rate proportional in each point of space and time to the optical intensity in the material:

$$G = \frac{\alpha_{IB}}{E_\gamma} I \tag{3-18}$$

3.1.2.2. Non-linear absorption

Focusing femtosecond laser pulses in a material can lead to very high optical intensities. When the electric field of the electromagnetic wave becomes non-negligible with respect to the local electric field in the medium, the polarization of the medium in response to the electromagnetic wave becomes non-linear and is expressed as a power series of the wave electric field *E*:

$$\mathrm{P} = \chi^{(1)}E + \chi^{(2)}E^2 + \chi^{(3)}E^3 + \cdots \tag{3-19}$$

where $\chi^{(n)}$ is the electromagnetic susceptibility of order n. The first term of this series is the linear polarization, with the imaginary part of $\chi^{(1)}$ being responsible for linear absorption. In a centro-symmetric medium like bulk silicon, the terms of even power of this series are null. The third-order term is at the origin of an absorption mechanism with a rate that is proportional to the square of the intensity: the two-photon absorption (TPA) [11]. The two-photon absorption coefficient β is related to the imaginary part of $\chi^{(3)}$ *by:*

$$\beta = \frac{6\pi}{4n_0\lambda_0} Im\left[\chi^{(3)}\right] \tag{3-20}$$

TPA requires the photon energy to be higher than half of the bandgap:

$$E_\gamma > E_g/2 \tag{3-21}$$

The generation rate induced by TPA is then given by:

$$G = \frac{\beta}{2E_\gamma} I^2 \quad (3\text{-}22)$$

When the condition (3-13) is verified, both linear interband and two-photon absorption can take place. The total generation rate is the sum of (3-18) and (3-22) contributions, although the linear mechanism is generally dominant in the energy range of interest for SEE laser testing.

When the condition (3-21) is verified but not (3-13), then the generation rate is given by (3-22), with a time and space distribution that is proportional to the square of the intensity distribution.

3.1.3. Other propagation mechanisms to consider

3.1.3.1. Material dispersion

A laser pulse is the result of the interference of a spectrum of waves with different wavelengths and different amplitudes. When these waves have a linear phase relationship, the pulse is said to be Fourier-transform limited, and the spectral width of the pulse is inversely proportional to the pulse duration. As an order of magnitude, the minimum spectral width of a 1ps pulse at 1064nm is 1.7nm.

The index of refraction of a material depends on the wavelength. Each spectral component of a pulse sees a slightly different index of refraction. This leads to a change in the phase relationship between the spectral components, which can lead to a change in the time-domain profile of the pulse. This is the dispersion mechanism. In particular, a pulse can either be stretched or compressed depending on 1) the curvature of the refraction index *n* as a function of wavelength around the central wavelength and 2) the length of the path it travels into the material. For an initially Fourier-transform limited pulse of duration τ_0, the duration after going through a thickness *z* of material is given by:

$$\tau(z) = \sqrt{\tau_0^2 + K^2 \frac{z^2}{\tau_0^2}} \text{ with } K = \frac{\lambda_0^3}{\pi c^2} \frac{d^2 n}{d\lambda^2}\Big|_{\lambda_0} \quad (3\text{-}23)$$

The dispersion length is commonly defined as the length after which the duration is increased by a factor $\sqrt{2}$:

$$L_D = \frac{\tau_0^2}{|K|} \quad (3\text{-}24)$$

The dispersion length in Si at 1064nm is around 1mm for 100fs pulses and 10cm for 1ps pulses. This means that, at 1064nm, dispersion in Si substrates with thicknesses below 1mm can be neglected for laser pulses of picosecond duration.

3.1.3.2. Plasma effect and self-absorption

The dense plasma of free carriers that can be generated by interband absorption of a laser pulse in a semiconductor can affect both the refraction index and the absorption coefficient of the material. This means that the propagation and absorption of the tail of a pulse can be affected by the free carriers generated by the front of the pulse. This is commonly called the plasma effect, although the part of the effect which concerns the absorption coefficient may also be called the self-absorption effect.

Given an estimation of the generated free carriers density, a first order approach for evaluating the plasma effect is to use the classical Drude-Lorentz model, which is known to provide a correct order of magnitude in silicon [12]:

$$\Delta n_{FC} = -\frac{e^2\lambda_0^2}{8\pi^2 c^2 \epsilon_0 n}\left(\frac{\Delta N_e}{m_{ce}} + \frac{\Delta N_h}{m_{ch}}\right)$$
$$\Delta \alpha_{FC} = \frac{e^3\lambda_0^2}{4\pi^2 c^3 \epsilon_0 n}\left(\frac{\Delta N_e}{m_{ce}^2\mu_e} + \frac{\Delta N_h}{m_{ch}^2\mu_h}\right) \quad (3\text{-}25)$$

where ΔN is the free carrier concentration, m_c the conductivity effective mass and μ the carrier mobility, with *e* and *h* subscripts referring to electron and hole quantities, respectively. Equations (3-25) can be used to estimate the plasma-induced effects on the beam propagation. Note that the plasma-induced index variation is negative. Since the generated carrier concentration is more important in the center of the beam than on its wings, the plasma-induced index variation distribution acts as a concave lens which tends to reduce the convergence of the beam and increases the beam-waist size. This effect is important to consider when modelling a laser pulse propagation in the substrate of a device.

3.1.3.3. Kerr effect

It was mentioned above that the third-order term in (3-19) is responsible for the two-photon absorption process. It is also at the origin of the Kerr effect, which introduces in the index of refraction a dependence on the optical intensity:

$$n = n_0 + n_2 I \quad \text{with } n_2 = \frac{3}{8n_0} Re\left[\chi^{(3)}\right] \quad (3\text{-}26)$$

where n_0 is the linear index of refraction. The radial and time profiles of the intensity will thus modulate the index of refraction and give rise respectively to self-focusing and self-phase modulation.

3.1.3.3.1. Self-focusing

Considering the Gaussian radial profile of the intensity and the positive value of n_2 in silicon, the center of the beam encounters a slightly higher index of refraction than the wings. This radial index distribution acts as a convex lens and leads to self-focusing of the beam. This effect is important to consider when modelling a laser pulse propagation in the substrate of a device, especially for sub-picosecond pulse durations.

3.1.3.3.2. Self-phase modulation

The Gaussian time profile of the intensity in (3-26) produces a variation of the index of refraction during the pulse. This leads to a phase modulation of the pulse that adds an additional spectral content to the pulse. This self-phase modulation is expected to become significant when the maximum phase excursion exceeds 2π, which in the plane wave approximation, leads to the following condition [11]:

$$I_0 \geq \frac{\lambda_0}{n_2 L} \quad (3\text{-}27)$$

where L is the length of the propagation medium. In Silicon devices, self-phase modulation is negligible for picosecond pulses in the useful range of pulse energies. It becomes significant for 100fs pulses with energies in the nJ range. An accurate modelling of its effects on the pulse deformation and propagation typically requires a non-linear electromagnetic solver.

3.2. The Single-Photon Absorption technique

The Single-Photon Absorption (SPA) version of the laser testing technique consists in using the linear interband absorption of the semiconductor to generate electron-hole pairs in the active layers of the DUT (fig. 3.5). This is the original variant of the technique developed in the early 90s [13]. It requires the use of photons with an energy that satisfies (3-13) and the induced generation rate is given by (3-18).

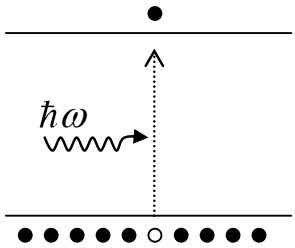

Fig. 3.5: principle of the Single Photon Absorption process

3.3. The Two-Photon Absorption technique

The TPA variant of the laser testing technique consists in generating electron-hole pairs in the active layers of the DUT by using the non-linear absorption mechanism described by (3-20) (fig.3.6) [14, 15]. The photon energy must satisfy (3-21) but not (3-13) and the induced generation rate is given by (3-22). Relying on a non-linear optics mechanism, this variant requires the use of laser pulses with a duration shorter than for SPA (see section 7.1.2).

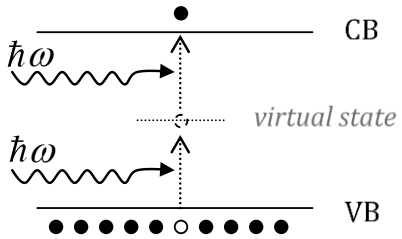

Fig. 3.6: principle of the Two Photon Absorption process

3.4. Front-side vs backside testing

Laser testing requires photons of the laser beam to reach the active semiconductor layer of the DUT. Historically, when devices had only a couple of interconnexion metal layers, laser testing was performed by focusing the beam through the front-side dielectric layers between metal interconnexions. This is the front-side approach (fig. 3.7).

At the wavelengths of interest for laser testing, a laser beam incident on an Al or Cu interconnexion will be reflected by more than 95% (see Table 3.1 above). The small fraction transmitted into the metal is absorbed in a few tens of nanometers (skin effect). In the end, the transmittance of a single metal line is always lower than 10^{-3}. Modern technologies have many-interconnexion layers and the areas that are not occupied by interconnexions are filled with passive metal cells (“dummies”) for planarization purpose. This makes the front-side approach impossible on most devices. The only notable exceptions where front-side testing might still be able to give partial results are:

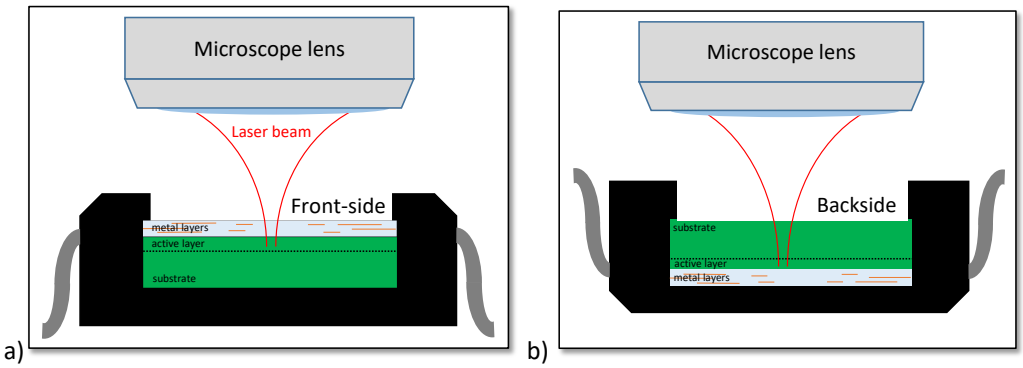

Fig. 3.7: principle of the a) front-side and b) backside laser testing approach

- Test vehicles specifically designed for front-side laser testing, in which the automatic inclusion of dummy cells has been explicitly excluded in the design phase [35],
- Commercial linear devices fabricated in old technologies using 1 or 2 low-density metal layers.

In these special cases, and depending on the goal of the test, it might be possible to obtain sufficient results from the front-side. However, it must be noted that metal layers may cover a fraction of the sensitive areas, possibly including the most sensitive regions.

The preferred approach for laser testing is to use the backside approach, in which the beam is focused through the substrate into the active layer (fig.3.7) [16]. In this approach, the attenuation of the beam by absorption as it propagates through the substrate must be considered.

Note that the front-side and backside terms refer to the sides of the die, not the package. The link between the die sides and the top and bottom sides of the package depends whether the die is packaged in a flip-chip configuration or not. In a flip-chip package, the backside of the die is accessible through the top side of the package.

Guideline #1

The preferred approach for laser testing is the backside approach, in which the beam is focused through the substrate into the active layer of the device.

While testing through the backside is the preferred approach, it may be impossible in some practical cases. In particular, non-flip-chip ball-grid array (BGA) packages are not compatible with backside laser testing.

Both front-side and backside approaches usually require specific sample preparation (see section 9) to enable optical access to the die.

3.5. Generic facility block diagram

Laser facilities can vary widely in their implementation, but they share some common features. Figure 3.8 presents the main components of a laser testing facility or beam line. A laser source produces the pulsed optical

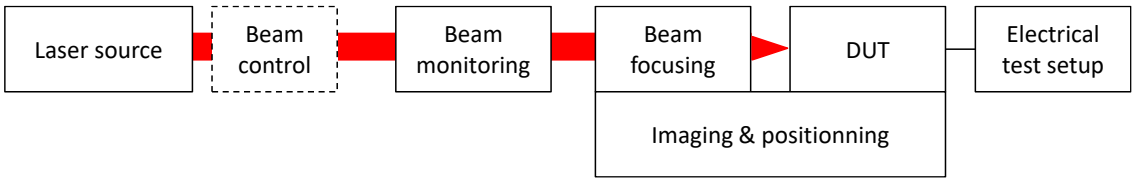

Fig. 3.8: main components of a laser testing beam-line and setup

beam and usually defines the wavelength and the pulse duration. Some parameters like the pulse frequency may be controlled from within the laser source or using external elements.

The beam line can be implemented either in free-space optics or using optical fibers. Free-space setups provide more flexibility but are more prone to long-term drift of beam parameters or alignment. Fibered setups provide improved long-term stability and optical safety.

The beam line should include in-line monitoring elements, at least for monitoring the laser pulse energy, as well as the beam profile for free-space setups. The beam is focused on the DUT usually by some kind of microscope that provides imaging and scanning capabilities to visualize and position the laser spot on the surface of the chip. The imaging system should provide different magnifications to observe the DUT with different fields of view, with at least one high-magnification lens to focus the laser beam during the test. Strong beam focusing is required to produce the smallest possible spot in the active region of the device in order to get as close as possible to the highly localized nature of the charge injection induced by an ionizing particle. The imaging system should include some sort of reticule to represent the position of the laser spot within the field of view.

For backside testing, a near-infrared light and camera are required in order to visualize the active layer through the substrate and to adjust the focus.

3.6. Typical steps of a laser testing campaign

Figure 3.9 presents the main steps of a typical laser testing campaign. Some steps will be detailed later in the document.

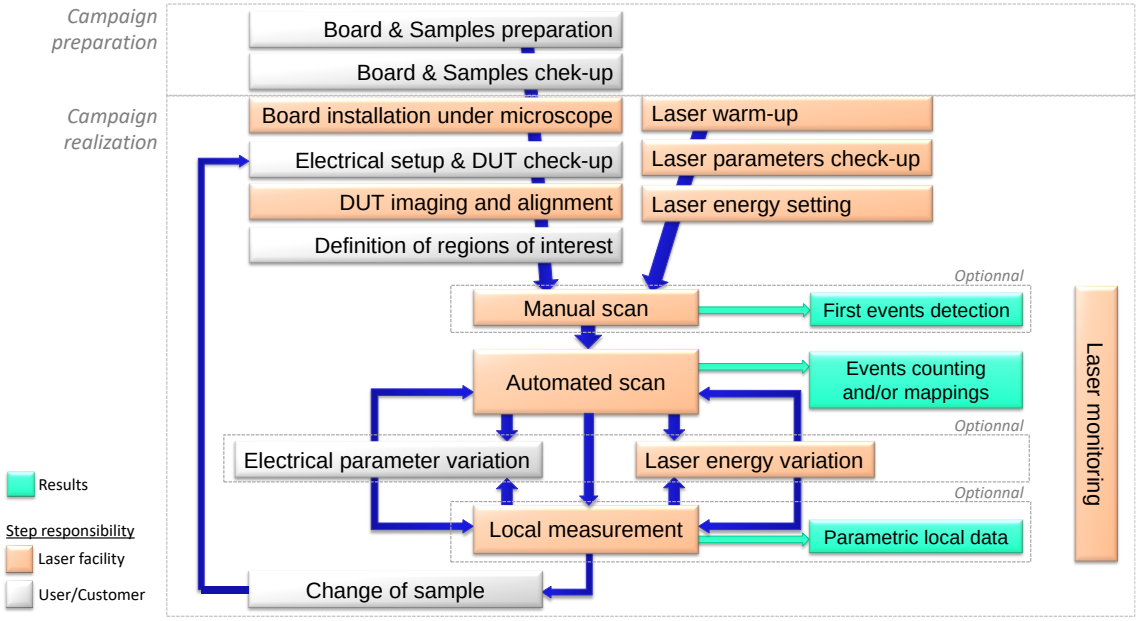

Fig. 3.9: main steps of a typical laser testing campaign

When the campaign is performed at an external facility, the responsible of each step of the campaign should be clearly defined prior to the campaign between the facility operator and the external user.

Guideline #2

When testing at an external facility, the responsibility of each step should be clearly attributed prior to the campaign to either the facility operator or the external user.

The campaign preparation steps are particularly important for a successful campaign. They are detailed in section 9.

The first step of the campaign itself consists in installing the DUT and its test board under the microscope (see constraints in section 9.2). Because the microscope objective lenses are fragile and expensive optical parts, during this step, great care should be put in preventing any contact between the lenses and the board, its components or cables, or the operator's fingers. Any contact with the optical part of the lenses or any mechanical shock to their metal housing can result in permanent degradation of the optical transmission or focusing quality.

Guideline #3

Nothing should make contact with the microscope lenses, either during the test board installation or during the scanning of the DUT.

The test board should be solidly attached to the beam line fixture using screws and/or spacers.

The next step is to make all the required electrical connections and to perform a complete check-up of the device operation to make sure that everything works properly after installation under the microscope. Although a laser facility is usually much less aggressive than a particle accelerator chamber in terms of electromagnetic environment, some experiments can require specific attention on the signal integrity to minimize the impact of noise sources like scanning stages or optical modulators. This is particularly the case for SET testing of analog and ultra-low power devices.

Guideline #4

The DUT and its test setup should be checked after installation on the beam line for signal integrity issues.

Once the board connections are completed and verified, it should be possible to adjust the position of the microscope lens with respect to the DUT and a first image of the DUT surface should be obtained.

The surface of the die should be inspected under low magnification with a large field of view to detect the presence of dust that may have been deposited during the sample manipulation since its preparation (see section 9.1). Big pieces of dust should be removed, for example using short pulses of pressurized dry air directed towards the surface, before proceeding.

Guideline #5

Large pieces of dust that are visible in the microscope image using a large field of view should be removed from the DUT surface.

Once the DUT surface appears to be clean, the microscope lens can be switched to the high magnification one. As explained in section 7.1.4, the vast majority of SEE testing should be performed using the high magnification lens, so the following adjustments should be performed using this lens.

In the case of backside testing, the focus of the imaging system should be translated into the substrate until an image of the active layers is obtained or the minimum safety distance between the lens and the DUT is reached. If the minimum safety distance is reached before any focused image could be obtained, the test can not be performed, and the DUT and/or the test board preparation should be reconsidered.

Once an image of the layer of interest is obtained, the orthogonality of the device with respect to the optical axis of the microscope should be adjusted (if the setup provides such possibility) in order to keep an acceptable

focus when translating through the regions of interest. The method for achieving this orthogonality varies with the facility optical and mechanical setup.

Guideline #6

The orthogonality of the DUT surface with respect to the optical axis of the microscope should be adjusted, typically by tilting the test board.

When mechanically possible, the X and Y axis of the scanning system should be aligned with the X and Y axis of the DUT, typically by rotating the test board fixture, in order to work with a unique system of coordinates.

The origin of the scanning system coordinates should be defined, for each sample, at an easily identifiable point of the image of the layer of interest that can be easily retrieved later. It is good practice to capture a snapshot of this origin point showing also the DUT orientation.

Guideline #7

The origin and orientation of the XYZ system of coordinates of the scanning system should be defined for each sample in a reproducible manner and visually verified using the imaging system. The position of the origin with respect to the DUT should be checked periodically during a campaign to detect and correct any mechanical drift.

The electrical test setup and acquisition system, as well as its interface with the beam line mapping software if needed (see section 6), must then be activated and tested.

The first events of interest are then classically located and identified by moving manually the laser position, and the laser parameters (mainly pulse energy and frequency) are adjusted to optimize the event rate. Once the sensitive regions of interest are identified, or if no event has been observed by manual scan, an automated scan can be launched to produce a systematic mapping.

4. Different test goals

The objective of each run of a laser testing campaign should be clearly defined among three generic goals that have increasing requirements on the test setup.

4.1. Events screening (Goal S)

Events screening consists in verifying the possibility of occurrence of a particular kind of event when irradiating the whole DUT or a specific region of interest.

This approach implies that capturing a unique event is sufficient and that keeping the track of the exact number of events with respect to the number of laser/DUT interactions is not required. This approach is useful, as examples, when dealing with destructive events or to validate the event capturing ability of a test setup.

4.2. Events counting (Goal C)

This goal consists in, at least, counting the number of occurrences of one or several kinds of events while also keeping the count of the number of laser pulses delivered to the DUT. At the same time, events details including waveforms or data logs may also be captured for each event. This approach is useful to calculate the probability of event occurrence, i.e. an event cross-section, and when the physical localization of the sensitive area on the DUT is not required. This goal requires an accurate control of the delivered pulse fluence. Depending on the test set-up, it might be necessary to estimate the cumulated dead-time of the test setup to calculate the effective pulse fluence.

4.3. Events mapping (Goal M)

Events mapping consists in capturing events and being able to attribute accurate 1D, 2D or 3D coordinates to each event in order to build a mapping of the DUT sensitivity. This goal requires the control of the coordinates of delivery of the laser pulses, and the possibility to establish a correspondence between the position of pulse delivery and the events acquisition by the test setup.

A mapping can be either:

- a quantity mapping: representing a quantity of interest, like a number of SEUs, the amplitude or duration of an SET, or a collected charge, as a function of the position.
- an event occurrence mapping: representing the occurrence or not of an event as a function of the position, or the occurrence of a binary event like an SEU. Such mapping can also be obtained from the first type by applying a filter or a threshold on the mapped quantity.
- a parametric mapping: representing the value of an experimental parameter, like the laser pulse energy or a supply voltage, to produce a particular kind of event.

Guideline #8

The goal of each run must be clearly defined between events screening, counting or mapping.

5. Comparison of SPA and TPA techniques

5.1. Main differences

SPA and TPA produce different distributions of electron-hole pairs in the semiconductor, as illustrated by fig. 5.1. The characteristics of those distributions and their implication for the technique are listed in table 5.1.

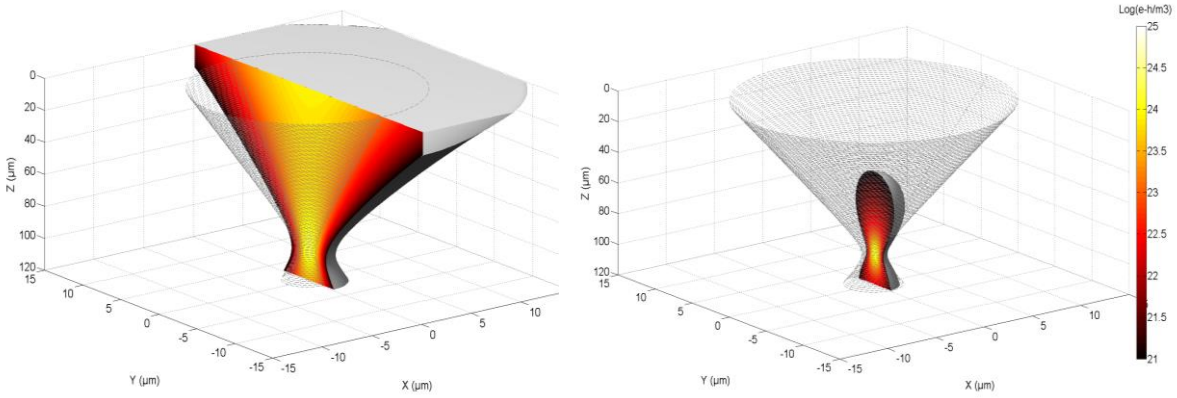

Fig. 5.1: Typical SPA (left) and TPA (right) induced charge distribution in a 100µm Si substrate

Table 5.1: comparison of SPA and TPA characteristics

Characteristic	**SPA**	**TPA**
Radial profile of charge track	*Gaussian of width* w_0	*Gaussian of width* $w_0/\sqrt{2}$
Longitudinal profile of charge track	*Dominated by convergence and exponential attenuation*	*Can be approximated by a Gaussian, limited to focal region*
Charge generation rate	*Proportional to optical intensity*	*Proportional to (optical intensity)²*
Charge quantity in a given volume	*Proportional to laser pulse energy*	*Proportional to (laser pulse energy)²*
Lateral (2D) resolution	*Reference value (depends on laser spot size, scanning step, energy resolution and stability…)*	*Slightly improved [17]*
Axial (3D) resolution	*No (> 10µm at a wavelength of 1064nm)*	*Yes, a few µm [15,18,19]*
Sensitivity to focus position with respect to the active layer	*Backside: Low* *Front-side: Low to high*	*High*
Sensitivity to backside surface quality	*Medium*	*High*

5.2. Preferred use cases

The SPA technique is the preferred default approach because it is less sensitive to focus variations and it is simpler to estimate the amount of charge injected.

The TPA technique is best suited in cases where its slightly better 2D resolution or its 3D resolution are exploited. Typical use cases include:

- finely-resolved scans of DSM technologies for goal M targeting small functions or design blocks, library cells or test structures.
- 3D analysis of bipolar technologies to resolve the depth of sensitive volumes.
- 3D analysis of power devices to resolve the depth of sensitive volumes.

6. Scanning modes

Typically, when testing under particle beams, particles are randomly distributed in space within the beam diameter and in time during the run. With laser testing, laser pulses can be triggered individually at a given position. Different strategies can then be used to produce a distribution of pulses in space and time, giving rise to different scanning modes.

6.1. Synchronous vs asynchronous scan

When scanning a device, three operations have to be performed that can either be synchronized or not:

1. Positioning: pointing the beam to the next position on the DUT
2. Laser pulse: delivering the laser pulse to the DUT
3. Acquisition: acquiring data from the DUT and correcting or resetting the DUT when required.

Several modes of scanning can be defined that cover most of practical cases and that differ by the fact that those three operations are synchronized or not.

6.1.1. Scan Mode A: Asynchronous scan and test

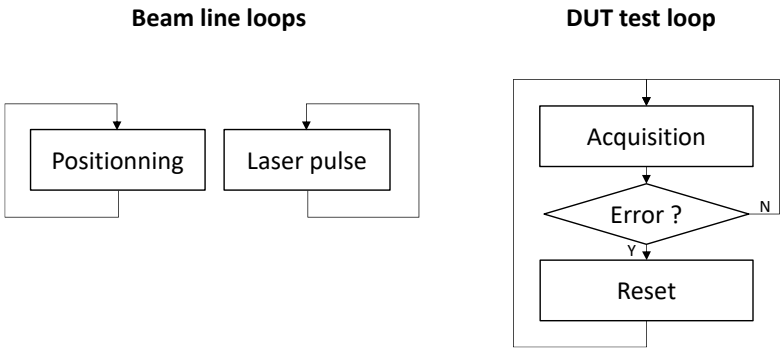

Fig. 6.1: Scan Mode A: Asynchronous scan and test

In this mode, the DUT is typically scanned continuously while delivering pulses at a constant frequency. Triggering of the laser pulses is not synchronized with the position. The DUT test loop is executed without any synchronization with the scan and pulses triggering.

6.1.2. Scan Mode B: Asynchronous test

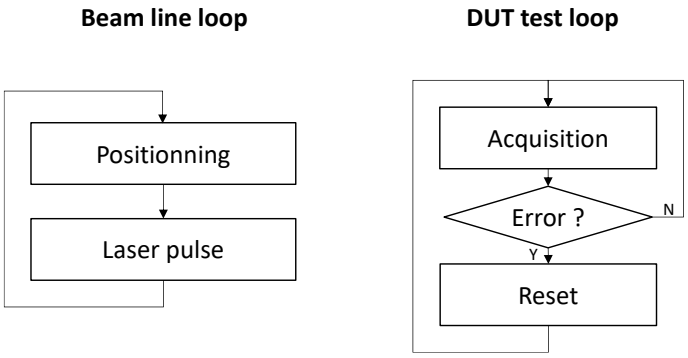

Fig. 6.2: Scan Mode B: Asynchronous test

In this mode, the scan motion and pulses triggering are synchronized, meaning that pulses are delivered at controlled coordinates. This guarantees the homogeneity of the distribution of the pulses over the scanned area. This distribution can be either random or based on a regular grid.

6.1.3. Scan Mode C: Synchronous test

In this mode, a synchronization dialog is established between the beam line loop and the DUT test loop to ensure that one pulse is triggered before each acquisition of the DUT response. In its simplest form, the "Pulse delivered" message can be a trigger signal from the beam line, while the "DUT ready" message might be replaced by a wait delay on the beam line side that should be long enough to account for all possible acquisition and reset durations on the DUT side. However, a tighter synchronization provides better results in terms of beam time optimization. Note that the synchronization that this scan mode refers to is only a macroscopic synchronization in the execution of the test flow on both sides (beam line and test setup).

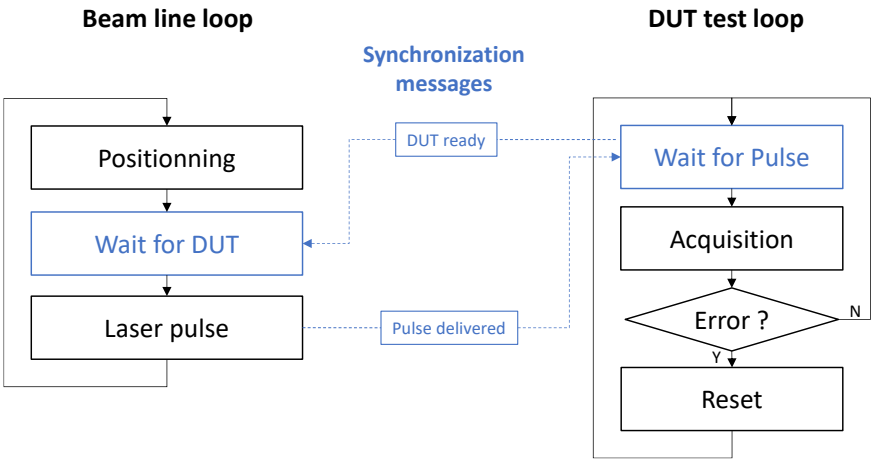

Fig. 6.3: Scan Mode C: Synchronous test

6.1.4. Scan Mode D: Time-resolved test

One step further in the synchronization consists in synchronizing the laser pulse arrival time on the DUT with a reference signal edge provided by the DUT test setup like, for example, a clock transition [20]. This micro-synchronization requires a more complex test setup and should only be used when such time resolution is needed.

6.1.5. Scan Mode selection

The selection of a scan mode is defined by considering the goal of the test, the available setup synchronization options and the required scanning time.

Scan modes A and B are simpler to implement as they do not require any connection between the beam line and the DUT test setup. They also provide results more rapidly than the other modes, especially for large ROIs.

Scan mode C is the preferred mode for Goal M, as it guarantees the event/position relationship. Scan mode B may also be used for Goal M with synchronous time-stamping of pulses and events.

Scan mode D is only used for time-resolved analysis either to extract a time window of vulnerability or to target a specific time window in the DUT operation.

Table 6.1: Scan modes vs Goal

Goal	S	C	M
Compatible Scan Modes	A, B, C, D	B, C, D	B, C, D
Preferred Scan Mode	B	B	C

Guideline #9
The scan mode must be defined in accordance with the test goal

6.2. Scanning motions

In order to scan the laser position through the regions of interest (ROIs), different type of motions can be involved.

6.2.1. Moving element

Fig. 6.4. illustrates the different elements that can be put in motion to perform the scan.

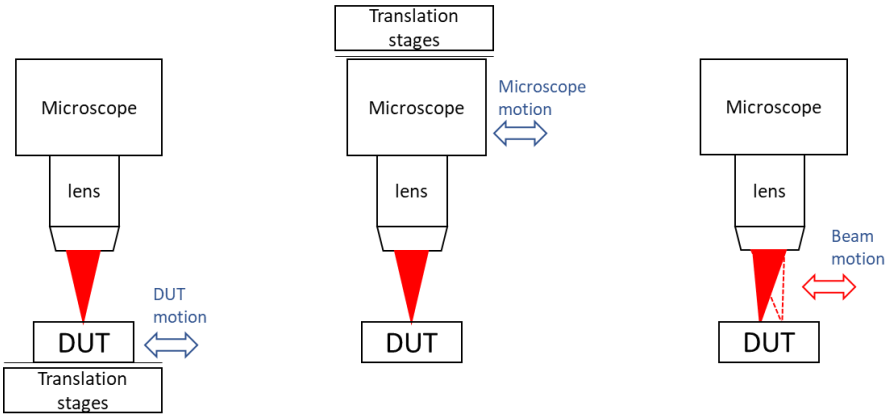

Fig. 6.2: different implementations of the scanning motion: DUT motion (left), Microscope motion (center), Beam motion (right)

Most facilities dedicated to SEE laser testing will move the DUT test board under a static laser beam. The main motivation for such setup, besides its simplicity, is that it ensures that the beam path and geometry don't change during the scan. This approach comes at the price of the mechanical inertia associated to the motion of the whole test board.

Some facilities will scan the whole microscope over or under a static DUT. This approach has larger mechanical inertia issues, but contrarily to the previous one, it is compatible with testing wafers or naked die under statically-positioned microprobes. In this approach, the laser system should be incorporated into or fiber-coupled into the microscope to prevent any variability of the laser injection into the microscope.

Some facilities, especially those focused on failure analysis tools, scan the beam through the microscope lens over or under a static DUT using a galvanometer-based steering mirrors optical setup. This approach suppresses the test board or microscope motion inertia issues, but it comes with two limitations. First, the region that can be scanned in a single run is limited to a fraction of the field of view of the high magnification lens. The field of

view has to be moved using one of the two previous approaches to cover the full die. Second, and most importantly, the beam path through the microscope optics and through the DUT substrate is slightly different for each scanned point [21]. This optical path variation is known to introduce small variations in the beam-waist size and peak intensity. While such variations are expected to be negligible for SPA on a well-designed system, this approach is not recommended for SEE testing with TPA due to the high sensitivity of TPA to the beam spot size and wavefront distortions.

Table 6.2: Compatibility of moving elements

Element in motion	Compatible laser technique		Compatible with microprobing
	SPA	**TPA**	
DUT	Yes	Yes	No
Microscope	Yes	Yes	Yes
Beam	Yes	Not recommended	Yes

Guideline #10

The scan motion must be compatible with the selected laser technique and the DUT electrical interface

6.2.2. Motion pace

Some facilities have the capability of scanning either in a step-by-step (SBS) mode or using a continuous-motion (CM) mode.

In SBS mode, the motion is stopped at each point of the scanning before triggering the laser pulse and acquiring the DUT response. This mode is particularly well-suited for goal M with test loops of long or irregular duration.

In CM mode, the scan of a line is typically performed by moving at a constant speed V from one edge of the ROI to the opposite one, while the laser pulses are triggered either at a constant frequency F or directly by the scanning stages at regular position intervals. When using a constant frequency triggering scheme, the maximum scanning step is given by V/F, and the reduced step between pulses on the edges due to the acceleration and deceleration phases has to be considered, for example by using additional margins in the definition of the ROI. The CM mode is usually more efficient in terms of beam time, and it reduces the mechanical vibrations associated with SBS mode repeated accelerations and decelerations between each position.

6.3. Scanning patterns

When scanning for goal M, the recommended scanning pattern consists in covering the ROI by a regular 2D grid defined by constant X and Y steps because the data it produces are easy to use and process. For mappings requiring the best resolution and repeatability, a motion pattern that compensates for any mechanical hysteresis of the scanning system is recommended.

For goal C, the laser pulses should be evenly distributed, i.e. delivered with a homogeneous density, over the ROI.

For goal S, any scanning pattern is acceptable.

7. Experimental parameters

7.1. Parameters definition, impact and recommended ranges

7.1.1. Wavelength

7.1.1.1. For SPA

For SPA, from equations (3-6) and (3-13), the wavelength must be shorter than 1100 nm to generate electron-hole pairs. The wavelength must be chosen so that the penetration depth is longer than the thickness of the active layers and the maximum extent of the charge collection mechanisms.

Recommended wavelengths for SPA in silicon are 1064nm and 1030 nm. They correspond to commonly available laser technologies and provide a penetration depth compatible with backside testing through thick substrates. From fig. 3.4 and equation (3.15), it can be estimated that the 1/e penetration depth (i.e. the depth at which the beam is attenuated by a factor 1/e) in a lightly doped substrate at those wavelengths is larger than 1mm.

Guideline #11

For SPA testing of silicon devices, the recommended wavelengths are 1064 nm or 1030 nm.

7.1.1.2. For TPA

For TPA, the wavelength must be comprised between 1150 nm and 2200 nm to generate electron-hole pairs in silicon by TPA. Commonly used wavelengths are 1260 nm, 1300 nm and 1550 nm. The first two are typically obtained using optical parametric amplifiers or oscillators in free space optical setups, while the third one is a very common wavelength of telecommunication systems and can also be obtained from fiber lasers. These wavelengths are compatible with backside testing through thick substrates. There is no practical motivation for using wavelengths longer than 1550 nm.

Guideline #12

For TPA testing of silicon devices, wavelength must be comprised between 1150 nm and 1550 nm.

7.1.2. Pulse duration

The time to consider when an ionizing particle interacts with a device is the sum of the time-of-flight through the active layers and the time needed for the generated carriers to thermalize through lattice interactions. The order-of-magnitude of this total time is in the 1 ps range. The laser pulse duration should also be shorter, or of the same order-of-magnitude as the local electrical function reaction time [22].

The minimum laser pulse duration available on a beam line is primarily defined by the laser source technology. In most cases, the pulse duration is not a parameter that can be easily modified by the user during a test campaign.

7.1.2.1. For SPA

For SPA, durations between 1ps and 50ps are commonly used. Using shorter durations is not recommended as it can lead to the appearance of non-linear propagation and absorption effects that complicate the estimation of the amount of injected charge.

Guideline #13

For SPA testing of silicon devices, the pulse duration must be selected in the sub-nanosecond range in accordance with the DUT performances. Commonly used values are between 1 ps and 50 ps.

7.1.2.2. For TPA

Sub-picosecond pulses are required to achieve sufficient peak intensities for TPA without requiring too large pulse energies. Durations between 100 fs and 500 fs are commonly used. With shorter pulse durations, non-linear propagation effects can become more present. For this reason, using durations shorter than 100fs is not recommended for SEE testing of silicon devices.

Guideline #14

For TPA testing of silicon devices, the pulse duration should be between 100 fs and 500 fs.

7.1.3. Pulse frequency

The laser pulse frequency (often referred to as the pulse repetition rate) is controlled either from within the laser source or using external modulators, and should be easily adjusted during a campaign.

The pulse frequency should be low enough to allow the DUT to return to a steady state between two consecutive pulses. Indeed, with laser testing, two consecutive pulses are usually delivered to very close positions on the DUT. If the pulse period is too short for the charge generated by one pulse to be completely evacuated (either by carrier collection or recombination) before the arrival of the next pulse, it can result in pulse-to-pulse accumulation of the generated charge and local heat leading to, in the best case, erroneous threshold measurements and, in the worst case, to a permanent thermal degradation of the device. Besides the carrier lifetime and the heat capacity of the tested structure, parasitic electric elements, trap capture and release times, and the local circuit response may also add to the total duration of the effect of a single laser pulse. For these reasons, when testing a DUT for the first time, the laser pulse frequency should be kept as low as possible and should never exceeds 1kHz.

The pulse frequency should be adjusted accordingly to the scan mode and scanning speed. When consecutive pulses are delivered at positions that are closer than twice the laser spot size, then the pulse frequency should be reduced so that the time between consecutive pulses prevents any accumulation of effects.

The pulse frequency should also be adjusted accordingly to the test sequence. Except for specific measurement scenarios, for instance when the response of the DUT has to be averaged over several pulses, it is usually preferred to have a single laser pulse delivered per test loop cycle, especially for goal M.

Guideline #15

Except for special circumstances, the laser pulse frequency should not exceed 1kHz and should be adjusted with respect to the scanning speed and the test loop frequency.

7.1.4. Beam spot size

In order to simulate the strongly localized interaction of an ionizing particle with a device, it is necessary to focus the laser beam as close as possible to the diffraction limit, using a high NA microscope objective lens. The smallest achievable laser beam-waist is then given by:

$$w_0 = M^2 \frac{\lambda_0}{\pi\, NA} \tag{7-1}$$

The laser spot size is defined either as the 1/e² diameter, noted d_{1/e^2}, or as the full-width at half-maximum (FWHM), noted d_{FWHM} of the intensity radial distribution, which are related to the beam-waist by:

$$d_{1/e^2} = \sqrt{2/\ln 2}\, d_{FWHM} = 2w_0 \quad (7\text{-}2)$$

It is recommended to use the 1/e² diameter definition as it englobes more of the pulse energy, although the FWHM definition is commonly encountered in an experimental context.

Standard high magnification microscope objective lenses used for SEE laser testing have an NA between 0.6 and 0.8, with a theoretical maximum of 1 when focusing in the air. Using high quality laser beams (with an M² close to 1), it is thus possible to achieve laser spots in the 1µm range for the NIR wavelengths commonly used for SEE testing.

The minimum laser spot size of a beam line is defined by the optical setup and wavelength. This is the spot size that should be used for SEE testing, especially where energy thresholds or cross section measurements are part of the goal. For SEE testing, a laser spot size below 1.8µm should be used.

Guideline #16

The laser spot size defined as the 1/e² diameter of the radial intensity profile should be smaller than 1.8µm.

Any larger spot size can be obtained either by defocusing, i.e. changing the distance between the DUT and the objective lens, or by using a lower NA lens. Working with larger spot sizes should be considered only as a first rough approach to identify possible sensitive regions of a DUT. It is important to note that using a larger spot size may give false positive as well as false negative results due to the different charge collection paths that can be brought into play when depositing the charge over a larger area. Also, the pulse energy required to trigger events generally increases with the spot size, increasing the risk of thermal degradation of the DUT.

Guideline #17

Using larger spot sizes is possible as a first approach, but it can lead to false negative or false positive results.

In free space optical setups, the laser spot size should be periodically monitored (see section 10.3).

7.1.5. Pulse energy

The laser pulse energy is the primary adjustable experimental variable during an SEE laser testing experiment. It is the sum of the individual energy of the photons that constitute the pulse. Although it has different units and physical meaning, the laser pulse energy plays a role similar to the LET in a heavy-ion experiment in the sense

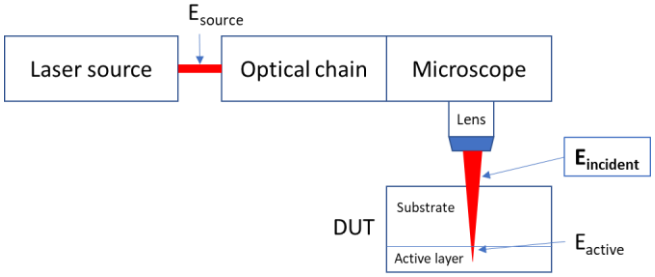

Fig. 7.1: Different laser pulse energy definitions

that it governs the amount of charge generated in the active layer of the DUT and it is usually possible to measure a threshold laser energy for which an SEE occurs.

The laser pulse energy can be measured or calculated at different positions along the optical path, as represented on Fig 7.1. The incident energy on the DUT is the only pertinent definition to use when reporting laser testing results. The energy in the active layer can be calculated from the incident energy.

Guideline #18

When defining or mentioning the laser pulse energy, it should be understood that it refers to the pulse energy incident on the beam entrance surface of the DUT.

7.1.6. Scanning resolution or Pulse fluence

- For goal M (mapping)

It is required to define the scanning resolution, i.e. the dimensions of the elementary pixel of the mapping. The scanning resolution is also commonly called the scanning step(s). The scanning resolution for a 2D mapping is commonly defined by setting *dx* and *dy*, the elementary steps of the scanning stages in the X and Y directions, respectively.

The scanning resolution has to be defined as a function of the desired resolution of the resulting mapping. The scanning resolution is also a key parameter to optimize the duration of a run.

The scanning resolution can be defined independently of the beam spot size. It is common to use scanning steps smaller than the spot size with pulse energies close to the energy threshold to achieve sub-spot-size resolution of fine structures. On the contrary, it is also common to use scanning steps much larger than the spot size when scanning larger ROIs, in which case it should be understood that the coverage of the DUT area is incomplete. In a first approach, large scanning steps can also be used in conjunction with a larger spot size (see guideline #17) to improve the coverage of the DUT area.

The respective step on each axis can be significantly different. It is common to use a fine step on one axis, and a much broader step on the other axis in order to optimize the beam time while still being able to resolve fine variations of the DUT response in one direction.

- For goals S (screening) and C (counting)

For these goals, one may only define a pulse fluence, which is the average number of laser pulses delivered per unit area.

Defining a target fluence instead of scanning steps relaxes the constraints on the spatial distribution of the pulses, enabling the use of different motion strategies like, for example, random walking across the die.

7.1.7. Pulse delay

The pulse delay is a parameter of interest only with scan mode D for experiments that aim to perform time-resolved analysis. It is defined as the delay between the time of arrival of the laser pulse on the DUT and a reference signal edge. Note that, because most laser facilities are based on free-running laser oscillators, an uncompressible jitter usually exists between the laser trigger signal and the laser pulse itself, which can limit the accessible time-resolution of a time-resolved analysis.

For all other types of experiment, the pulse delay is left undefined, taking a random value for each pulse. This reproduces the clock cycle coverage that is naturally obtained during particle broad beam testing with particles striking the DUT at random instants.

7.2. The effect of temperature

Variations in the temperature of the beam-line room can have various consequences on the beam line, especially during long runs, including:

- Impact on the laser source operation and energy stability
- Beam pointing variations in free-space optical setups
- Dilatation of the mechanical stages, the test board fixture and the microscope

Guideline #19

The temperature of the beam-line room should be actively stabilized.

The temperature of the DUT die has an impact on all the physical quantities involved in the laser beam propagation and the photon absorption:

- Effect on the index of refraction: the index of refraction of silicon increases with temperature [23, 24, 25]. A temperature gradient in the substrate acts as a complex thermal lens on the beam propagation leading to an offset in the optimal focus position.
- Effect on the absorption coefficient: both interband and free-carrier absorptions increase with temperature [26].
- Effect on the optical path in the device due to thermal expansion.

In practice, die temperature fluctuations of a few degrees can be estimated to be of second-order in front of other sources of variability in the DUT response. However, with DUTs that present significant self-heating, the die temperature can change by several tens of degrees from the initial room temperature to the operational temperature that is reached after the DUT has been fully powered and exercised by the test setup for a certain amount of time. In this case, the test sequence should include a warm-up phase so that such variations do not occur during a measurement run.

Note that the DUT die temperature also has an impact on the charge collection mechanisms and the circuit response, but this is out of the scope of this document. The die temperature might be controlled using additional heating or cooling elements on the test board as a part of the experiment, typically when exploring the sensitivity to SEL. Similarly, the temperature should be stabilized and the focus adjusted before any laser testing measurement.

Guideline #20

The temperature of the DUT die should be stabilized before each run to prevent uncontrolled variations in the laser propagation and charge generation mechanisms.

8. Test plan definition

8.1. Definition of the regions of interest

For DUTs that exceed a few mm², it is usually neither needed nor realistic to scan the whole die with the finest resolution, especially with the longer test loops. Scanning larger DUTs in a single run is possible but, depending on the test loop duration, it may be required to increase the scanning step to complete the run in a reasonable amount of time. Dividing the chip surface in smaller ROIs allows one to adapt either the scanning resolution, the test sequence or the scanning mode for each ROI. Definition of the ROIs is the result of a trade-off between the desired coverage of the die, the required resolution or target fluence in the different regions and the available beam time.

In most cases, a ROI is a rectangle that is defined by its coordinates with respect to a fiducial point on the DUT taken as the origin. Defining an ROI thus requires either the DUT layout, a scaled schematic of the DUT floorplan, or a backside infrared picture of the DUT ideally taken after sample preparation.

Visible symmetries or repetitions in the DUT floorplan may be used to reduce the number or the size of the ROIs, but this should only be considered with a deep understanding of the DUT layout organization and functioning, because there could be undocumented and invisible design variations from one block to a similarly-looking one.

When defining an ROI to target a specific design block of the DUT, it is wise to include a margin of a few µm on each side to observe possible extensions of the sensitive areas beyond the frontiers of the block.

8.2. Pulse fluence

The pulse fluence is the number of pulses delivered per unit area.

For goals S and C, defining a target pulse fluence can be envisioned similarly to the specification of a fluence for a heavy ion irradiation campaign. Increasing the fluence provides a better coverage in space and time of rare events that have a low cross section related either to a small sensitive area or a short vulnerability window.

8.3. Beam time estimation

The time required to scan a large DUT with high resolution should not be underestimated. It is highly dependent on, first, the required accuracy in terms of event counting and mapping and, second, the duration of the test loop. In particular, it is important to determine if the scan should be interrupted while executing the test loop (scan mode C), since the scanning time can be significantly reduced for goals S and C using scan modes A or B.

Considering the area to be scanned *S*, the desired resolution *r*, and the average scanning speed *v* that can be safely achieved without generating vibrations at acceleration and deceleration, a rough estimation of the scan duration for goal M in scan mode C is given by:

$$t_{scan} \approx \frac{S}{r^2}\left(\max(t_{test}, t_{laser}) + \frac{r}{v}\right) \quad (8\text{-}1)$$

where t_{test} is the test loop duration and t_{laser} is the minimum laser pulse period, assuming that the test loop has to be executed after each laser pulse and that the motion is interrupted at each point.

9. Test setup preparation

9.1. Samples preparation

9.1.1. For front-side testing

Front-side testing should only be envisioned with the limitations mentioned in 3.4. Note that front-side testing of flip-chip packaged devices is not possible.

Preparation for front-side testing requires package opening, including the removal of any polyimide layer if present on the top of the BEOL, to provide optical access to the top dielectric layer. For plastic packages, this is usually performed by a local chemical attack of the plastic.

9.1.2. For backside testing

Sample preparation for backside laser testing is made of the following steps:

1. Required: optical access to the backside of the die

   This step requires opening of the package, similarly to what should be done for backside heavy ion testing.

   If the DUT has an electrode or a metallic thermal pad on the backside, a local aperture should be performed using a micro-drilling tool. The local aperture should preserve enough of the electrode area to maintain its electrical function. The dimensions of the aperture must be sufficient to prevent any clipping of the beam when scanning across the ROIs.

2. Optional: substrate thinning
   In most cases, substrate thinning is not required for laser testing, providing the laser pulse energy can be increased sufficiently to compensate for absorption by the substrate. Thinning down to 100 µm or less might be required only for thick and heavily doped substrates. A simple test could be performed using a standard near-infrared microscope: if the DUT structures can be observed with a good contrast through the substrate, then thinning the substrate is most probably not required.
   When thinning is performed, the homogeneity of the remaining thickness across the die is a critical parameter.
3. Required: optical-grade quality polishing of the backside surface of the substrate
   This step is an addition to the classical preparation for backside heavy ion testing. It has two objectives: first, to prevent significant distortion of the laser beam wavefront that would dramatically impact the focused spot size, and second, to enable the visualization of the DUT structures through the substrate using a near-infrared camera.
   This step is typically performed using a micro-drilling tool equipped with cotton tips and an abrasive paste.
   A visual inspection using a microscope should be performed to detect significant defects in the preparation.
   A standard requirement for qualifying a surface of optical-grade is a residual roughness smaller than $\lambda/10$ over the field dimensions. In the case of laser testing, this could be translated into a residual roughness of the backside surface smaller than 100nm within circles of 50µm. However, sample preparation facilities are often not equipped for verifying this residual roughness with a sufficient resolution. As a simple test, one may observe the projection on a sheet of paper of the reflection

of a laser pointer beam incident at 45° on the backside surface. The observed spot should be clean from speckle.

Note that even if the substrate was not thinned in step 2, the step 3 is required to clean the backside from any material deposition that may have occurred during the fabrication or packaging process.

Guideline #21

Sample preparation for backside laser testing must include the optical polishing of the backside surface.

9.2. Constraints on test-board design

9.2.1. Optical access

The test board should provide easy access to the DUT die. The DUT surroundings on the PCB should be clear of any component or connectors higher than the working distance of the lens, which is typically around 10mm for high magnification lenses. The minimum volume that should be completely clear of anything is related to the diameter of the objective lens ϕ and the maximum dimension of the die *W*, as represented in fig 9.1. This minimum clear volume should only be used when deep sockets or a heat dissipator are required. When possible, the recommended volume that should be clear of components includes an additional margin of 5mm and an extended cone to reduce the risk of accidental contact with the lens when the lens approaches the DUT.

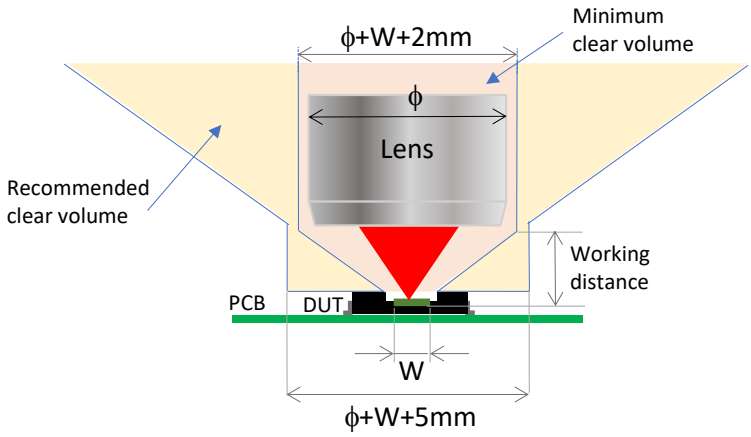

Fig. 9.1: Required volume for optical approach of the DUT

Guideline #22

The test board must have a volume clear of any element around the DUT to enable the approach of the microscope objective lens.

For backside testing of non-flip-chip packaged devices, a hole in the PCB supporting the DUT is often required. This hole should be larger than the die to prevent any clipping of the laser light cone when the beam is positioned on the edge of the die, as represented in fig 9.2. The light cone half angle θ is related to the numerical aperture (NA) of the lens. The required margin *m* to be considered on all sides of the hole can be estimated by:

$$m \approx h \frac{NA}{\sqrt{1-NA^2}} + 1\text{mm} \quad (9\text{-}1)$$

where *h* is defined on fig 9.2 as the height between the lens side of the PCB and the active layer of the die, and the additional 1mm is a margin to account for package-to-PCB assembly positioning errors.

Guideline #23
The laser light cone must not be clipped by the DUT package, socket or test board.

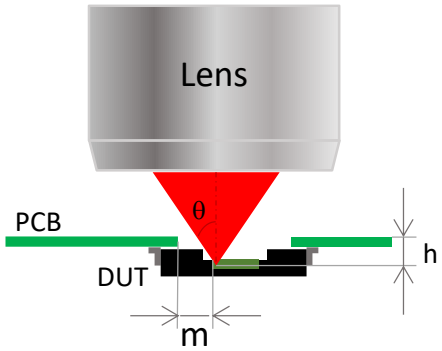

Fig. 9.2: Through-PCB backside testing

9.2.1. DUT position on the board

Once the board is attached to the beam line fixture, all the ROIs of the DUT must be within the range of the scanning system. The fixture geometry and the scanning system range vary from one facility to another. In some cases, an intermediate plate might be used, which is fixed on one side to the fixture and on the other side to the PCB holes, which can help in positioning the DUT within the scanning range.

When designing a test board specifically for laser testing, it is a good practice to position the DUT at the center of the board.

9.2.2. Mechanical stability

Mechanical stability of the test board is a strong requirement to ensure repeatable positioning and focusing of the beam during the campaign. Significant efforts should be put in designing a mechanically stable test board in the campaign preparation phase. Note that daughter boards that connect to their mother-board by a single connector, can be particularly unstable.

The test board should not embed any source of continuous or episodic vibrations, including:

- any active fan. When required, a gentle air flow should be generated from a fixed point off the board.
- manual switches that need to be regularly operated during the campaign.
- high power mechanical relays.

When visualizing the DUT with the microscope and a high magnification lens, every effort should be made to reduce any observable vibration.

Guideline #24
The test board should not embed any source of continuous or episodic vibrations.

9.3. Test equipment requirements

9.3.1. Constraints on cables

Connections between the test board and the rest of the electrical test setup should be designed in order to:

- prevent the propagation of vibrations from the equipment (power supplies, oscilloscope…) to the test board.
- prevent the application of strong mechanical constraints to the test board, especially when scanning by DUT motion.

This can be achieved using light and flexible enough cables.

The weight of long or heavy cables should be supported, while still allowing free/unconstrained movement of the test board.

9.3.2. Test loop and/or data acquisition synchronization

If scan modes C or D are required, the DUT test loop needs to be synchronized with the beam-line loop using the appropriate signals and connections.

When testing for goal M, the DUT test loop usually needs to provide some form of data, representing the information to be mapped, to the beam-line scanning software that is typically also in charge of building the mapping. In its simplest form, this data can be a binary event signal that can be acquired using an analog input or an oscilloscope of the beam-line. Alternatively, the DUT test loop could retrieve in real-time from the beam-line the laser position corresponding to each data acquisition in order to build the map.

10. Test realization

10.1. Laser safety

Most pulsed laser sources used for SEE laser testing fall in the laser safety Class 4 as defined by the IEC 60825 standard, which is the most dangerous class of lasers. When such lasers are used in free-space optical setups, wearing laser protection goggles at all times is mandatory to prevent the risk of retina burn in case of direct or indirect exposure to the beam and, depending on local regulations, a laser safety training might be required to approach the beam line.

Some facilities use fiber-guided beams from the source to the microscope and/or an interlock circuit to turn off the laser when the user might be exposed (for example when opening the door of an equipment). With such implementation, the laser testing system may fall in the laser safety Class 1, meaning that the laser system is safe under all conditions of normal use.

In all cases, users should be informed of the class of the laser beam line and follow the appropriate regulations.

Guideline #25
Users must follow the laser safety regulations of the facility.

10.2. Beam parameters monitoring

Some beam line parameters should be monitored during the campaign.

The laser pulse energy should be monitored periodically for long-term drift. As an example, room temperature variations may affect the output power of some laser sources or the calibration of power measurement systems.

Guideline #26
The laser pulse energy should be periodically monitored and recorded.

Pulse-to-pulse variations of the laser pulse energy might be monitored only when it may significantly affect the results of the test. Some laser source technologies, like Q-switched cavities, are more prone to producing such variations than others. An excessive pulse-to-pulse variation of the pulse energy will manifest itself in the form of a noisy mapping or with events being difficult to reproduce near the threshold energy. Pulse-to-pulse variations of the laser pulse energy will have a higher impact on TPA than on SPA, due to the quadratic relationship between the pulse energy and the generated charge with TPA. One way to deal with such variations is to acquire the signal from a photodiode that receives a fraction of the beam for each pulse delivered to the DUT and to correlate each test result with this acquisition.

In free-space optical setups, the laser spot size should be periodically monitored for long-term drift, especially for TPA testing, because this parameter has a strong impact on the charge generation. The absolute characterization of a laser spot size near the diffraction limit is not trivial and requires a specific optical setup. Thus, a relative monitoring can be performed by measuring the TPA-induced signal in a photodiode.

Guideline #27
The focused laser spot size of a free-space optical setup should be periodically monitored and recorded.

10.3. Focus adjustment

The initial focus adjustment, before any run is started, usually consists in positioning the beam-waist along the microscope axis in the active layer of the DUT in the region of interest by adjusting the distance between the microscope lens and the DUT. If the laser beam injection into the microscope is ideally set up, this should correspond to the focus position that produces the optimal image of that layer.

Several phenomena can affect the focus positioning during the scan:

- residual default of orthogonality of the DUT with respect to the optical axis
- inhomogeneous thinning of the substrate
- mechanical constraints imposed by the cables on the test board
- thermal dilatation of the die, package or test board
- thermal lens within the substrate

Countering these effects may require a periodic adjustment of the focus during a run. When real-time adjustment is not possible, then the ROI should be divided in smaller regions in which an optimal focus positioning can be maintained.

The tolerance for focus adjustment depends on the absorption mechanism and on the DUT technology. TPA is more sensitive than SPA to an offset of the focus position, due to the longitudinal profile of the induced charge distribution. SOI technologies are more sensitive than bulk technologies to an offset of the focus position due to their different charge collection volumes. Similarly, highly integrated CMOS technologies are more sensitive than power technologies.

The tolerance for focus adjustment also depends on the goal of the run and the pulse energy level with respect to the threshold energy for generating events. As an example, for goals S and C using a pulse energy that is known to be twice the threshold energy for the events of interest, the tolerance on focus adjustment is much higher than for goal M with a pulse energy just 10% higher than the threshold energy.

As an order of magnitude, the tolerance on the focus adjustment should be ±1µm whenever possible. Depending on the technology, the goal and the energy, such tolerance may already lead to measurable variations in the response of the DUT, in which case the analysis of the results should consider the focus position as a source of data variability.

Guideline #28

The position of the beam-waist along the microscope axis with respect to the DUT should be maintained in the active layer of the DUT during the scans, with a tolerance that should be defined as a function of the test goal and parameters.

Once an SEE sensitive area has been identified on a device, its sensitivity to focus adjustment can be estimated by doing local measurements of the SEE threshold energy as a function of the focus position.

10.4. Determining the energy range of interest

Determining the threshold energy E_{th} for generating events of interest is often an important part of a laser testing campaign, not only for knowing the value itself but also to identify the energy range of interest. Depending on the type of SEE, the device technology, its substrate thickness and the laser wavelength, the threshold energy can range from a few femtojoules to a few tens of nanojoules.

For non-destructive events, figure 10.1 presents one of the possible methods for determining the threshold energy. This method is given as a basis for new users of the laser testing technique. Depending on the specificities of the experiment and the experience of the users, other methods might also be pertinent.

The method first requires the definition of an ROI that is expected to produce the events of interest. Without any information on the DUT, this ROI might be the full die, but in order to save the beam time, this ROI should be reduced to the minimum area using the available knowledge of the device floorplan and the observable repetition of the structures.

In order to reduce the risk of laser-induced degradation (see section 13.5), it is recommended to perform the first scan using a low pulse energy E_{start}. When previous data are available on a similar device and technology, they should be used to estimate a lower bound of the energy range of interest and use this value as E_{start}. If a threshold LET has been obtained from particle-beam testing, the pulse energy giving the same equivalent LET might be calculated for SPA using section 14.2 and should be used as E_{start}. With a DUT for which no information on the sensitivity is available, the values in table 10.1 can be used as a starting point when testing with SPA at 1064nm.

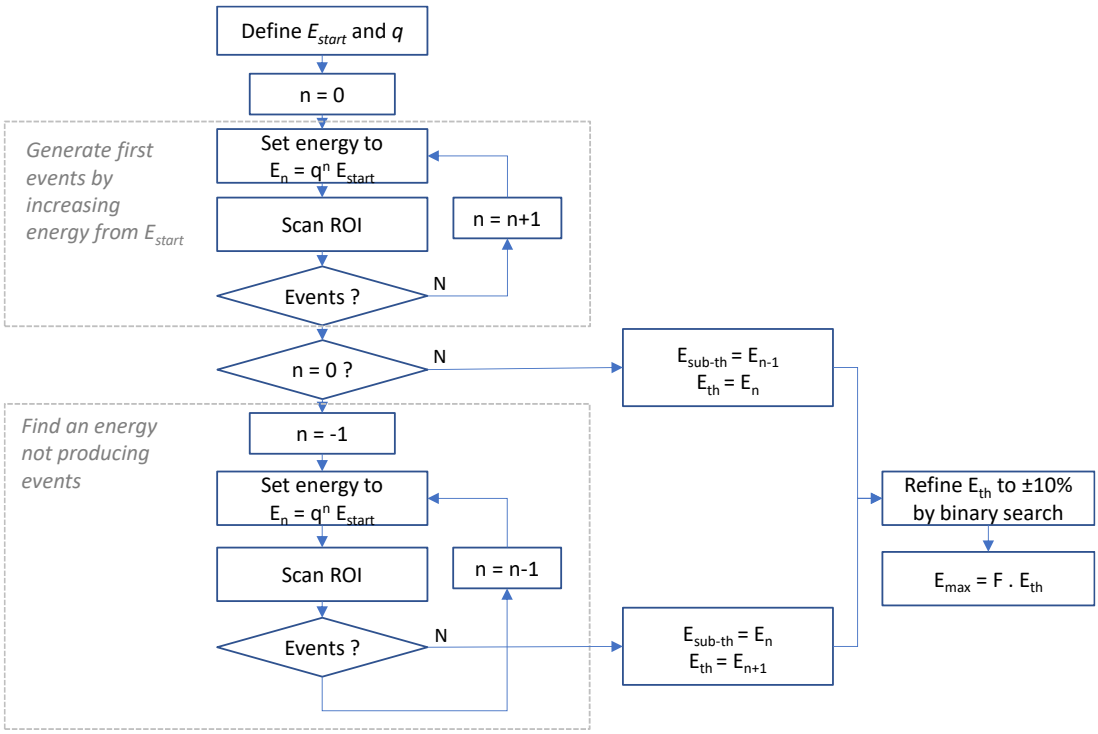

Fig. 10.1: A method for determining the pulse energy threshold and useful range

Once E_{start} is defined, the method consists in repeating the same scan while progressively increasing the energy in a geometric series until the first events are observed, using for the n^{th} scan an energy $E_n = q^n E_{start}$, with q comprised between 2 and 3.

If events are already observed during the first scan at E_{start}, then a sub-threshold energy E_{sub-th} should be researched by reducing the energy, using for the n^{th} scan an energy $E_n = E_{start} / q^n$.

Once first values of the sub-threshold and threshold energies are identified, the threshold energy should be refined between those two initial values by binary search until an accuracy of 10% is reached.

When destruction of the DUT by laser-induced degradation is a strong concern, a maximum energy E_{max} to be used can then be defined as the threshold energy multiplied by a factor F. Safe values of F are extremely dependent on the DUT technology, its design margins, and the laser parameters. Table 10.1 gives typical orders of magnitude when testing with SPA at 1064nm, but it is important to note that outliers are always possible in the sense that some technologies may either support higher values or present some degradation at lower values of F.

Table 10.1: method parameters for SPA testing with a wavelength of 1064nm for different technology families

DUT technology	E_{start} (pJ)	q	F
Deep sub-micron CMOS	1	3	50
Older CMOS	10	2	100
Linear or power device	20	2	200

11. Test report

11.1. Required parameters

A laser testing report should include all the necessary information to repeat the experiment and to compare with results obtained using other test methods or facilities. Also, the report should capture the information that could lead to identifying unexpected bias in the experiments.

A template test sheet is included in Annex 1.

11.2. Energy measurements

The laser pulse energy values presented in a test report must refer to the incident energy (guideline 18). When possible, the report should indicate how those values are measured and/or calculated in order to enable future corrections in case a bias in the energy measurement or calculation method is detected. In addition, any calculations used to determine the pulse energy at the active layer, and/or the charge deposited in the sensitive volume, should be described in detail, using the incident energy as the point of reference.

11.3. Laser cross section

The laser cross section is a measurement of the sensitive area of a device for a specific set of test conditions and beam parameters.

For goal C, it is defined in a statistical manner similar to the one used for broad-beam experiments. Given Φ, the effective laser pulse fluence over the ROI, and N, the number of detected events of interest, the laser cross section for these events is defined by:

$$\sigma_L = N/\Phi \tag{11-1}$$

When scanning a 2D ROI for goal M with constant scanning steps *dx* and *dy*, an equivalent geometrical definition is given by:

$$\sigma_L = N\ s \tag{11-2}$$

where *s=dx.dy* is the area of the elementary “pixel” of the mapping.

When reporting the sensitive area, the results should be referred to as “Laser cross section” instead of just “Cross section” to prevent any confusion with particle broad-beam results.

11.4. Mappings

The presentation of mappings should always include the scanning conditions, including the scanning mode, scanning steps and laser frequency, to enable the interpretation of possible scanning artefacts. A color scale is required for non-binary mappings.

12. Use cases examples

This section reviews the specifics of common use cases of laser testing.

12.1. SET testing of a linear device

SET testing of a linear device is usually characterized by the following specific points:

- One or several analog signals from the DUT are monitored for the occurrence of SET using an oscilloscope. The oscilloscope acquisition should be triggered by an edge provided by the laser beam line that is synchronous with the laser pulse. This is required for goal M. For goals S and C, the oscilloscope may also be triggered by the SET, in which case the trigger threshold should be carefully adjusted to prevent false positives as well as missing pertinent events.
- The delay of propagation of the SET from the point in the circuit where it is generated to the monitored signal on which it is observed is, in most cases, deterministic and related to the DUT operating bandwidth. If the oscilloscope acquisition is triggered by a laser pulse synchronous signal, the oscilloscope acquisition window delay (oscilloscope trigger delay) and width (oscilloscope time base) must be adjusted to ensure that the SET is captured within the acquisition window.
- The shape of the SET, including its amplitude and/or duration, varies continuously with the laser pulse energy above a certain threshold related to the circuit functions or the signal acquisition resolution. The oscilloscope vertical and horizontal scales should be adjusted to cover the ranges of possible amplitudes and durations.
- The thickness of the sensitive active layer of linear devices can exceed a few µm, and the shape of the SET may vary as a function of the beam-waist position within this thickness, especially with the TPA technique. At least one run should be devoted to the acquisition of the SET shape as a function of the focus position at a sensitive location. If reference SET shapes obtained under particle beams are available, the position of the laser beam-waist on the focus axis should then be adjusted to produce SET shapes that are as close as possible from the reference ones. In the absence of reference shapes, the laser beam-waist should be positioned by default at the depth that produces the SET of maximum amplitude. This default focus position can change between different regions of the DUT, especially with bipolar technologies.

12.2. SEL screening of a CMOS integrated circuit

This use case typically aims at defining if a device may or may not suffer from latchup when exposed to heavy ions. In a first approach, the searched response is either yes or no. When the answer is yes, a refined response may include an SEL laser energy threshold measurement and an estimation of the SEL cross section.

This use case falls in the goal S category and should use scan modes A or B. The DUT test setup should include an overcurrent detection and protection system on each of the DUT power supplies. The temperature of the die should be stabilized before the beginning of the runs.

Screening a device for SEL requires scanning the entirety of the DUT chip. Because of its higher tolerance to focus variations when scanning large areas, and also because of its longer charge track extension in the substrate, the SPA technique is the preferred one for SEL screening.

The laser pulse energy should be high enough to maximize the probability of triggering events, although the risk of laser-induced degradation should be carefully considered. A starting value of the laser pulse energy could be obtained by calculating (see section 14) the energy corresponding to an equivalent LET of 100MeV.mg^{-1}.cm^2. Ideally, the supply currents should be continuously monitored and logged in order to observe any drift of the

supply currents (below the SEL detection threshold) that could be the signature of laser-induced degradation or the consequence of other types of events.

The laser pulse fluence should be high enough to provide the required coverage of the different scales of design structures in the DUT. A common approach is to perform a first scan with large steps (e.g. 10µm) and to refine only in the absence of events. A non-minimal spot size might be used in this first approach (see guideline #17).

12.3. SEU/MCU/MBU/SEFI testing of a memory device

Memory devices are characterized by the fact that the majority of their surface is occupied by the array of memory cells, divided in a hierarchy of blocks. The various levels of symmetry of the DUT floorplan can be used to adjust the size and the scanning resolution of the ROIs in order to reduce the beam time. Some ROIs should also be positioned randomly on the DUT to detect variations of the sensitivity that are not simply related to the device floorplan.

With SRAM devices, the first runs should be dedicated to the determination of the energy threshold for SEU of memory cells in ROIs located at different positions in the array, using the method in 7.1.5. Considering the dense repetition of the memory cells, each of these ROI could be limited to a small fraction of the smallest identifiable block. In this phase, the synchronization of the DUT test loop with the scanning is not strictly required and the scan modes A or B can be used. When possible, the laser pulses should be delivered while the cells are in storing mode, i.e. not accessed for read or write. With DSM technologies, note that the energy threshold difference between the observation of SEU and MCU can be difficult to determine and require a good stability of the laser energy and the mechanical setup. One common way to deal with repeatability issues is to average the results of repeated scans realized in the same conditions.

For goal M, the scan mode C is the preferred one. Thus, the time required by the DUT test setup to verify the integrity of the stored pattern in the memory array is a critical point to optimize in order to reduce the total scanning time. The logical mask and range of tested addresses should be optimized according to the ROI.

12.4. SEB testing of a power device

When the objective is only screening for SEB at a given supply voltage, the same method as described above for SEL screening could be used. However, in most cases, an estimation of the safe operating area (SOA), of the device cross section and of its sensitive depth are part of the expected results. Testing for destructive SEEs is not only costly in terms of the required number of prepared samples but it also takes time for replacing and repositioning the DUT each time a sample is destroyed. For these reasons, a common method consists in getting as much information as possible in a non-destructive mode [27], then verifying the occurrence of destructive events only for a limited set of conditions.

Considering SEB testing of an Si MOSFET device, a non-destructive mode is typically achieved by:

- adding a series resistor between the drain and the high-voltage power supply,
- not adding a “charge reservoir” capacitor between the drain and the ground,
- starting the test with low values for the drain voltage (<30% Vmax).

In these conditions, it should be possible to observe, with an oscilloscope probe on the drain, laser-induced SETs that don’t result in the device destruction. Note that the expected amplitude of such transients is typically in the mV range due to the high capacitance of power devices electrodes. A typical test plan would then explore the dependence of those non-destructive SETs on the laser position in both the XY plane and the Z direction in order to identify the laser position that produces either the maximum transient amplitude or the maximum collected charge. A small ROI of a few µm² can then be defined around this position, which should be scanned

repeatedly with increasing pulse energies to cover the energy range of interest. The ROI should be regularly shifted along the repetitive structure to prevent laser degradation accumulation in the same region. This energy ramp will then be repeated with increasing drain voltages, until either a destruction occurs or changes appear in the relationship between the laser energy and the collected charge that could be the signature of the triggering of an avalanche phenomenon.

12.5. SEE testing of a programmable SoC

SEE testing of a programmable SoC is usually characterized by the following points:

- The DUT is composed of different types of resources. The test coverage strongly depends on the test setup, including the configuration of the SoC and the benchmarks or application codes executed by the SoC.
- A fraction of the DUT, if not all, operates at high frequencies, leading to self-heating of the DUT. The test sequence should be arranged to prevent strong fluctuations of the die temperature during a laser test run. Some situations may require the use of an active cooling of the DUT that preserves the optical access to the backside.
- The chip area is large and has to be divided in multiple ROIs to achieve and maintain a correct adjustment of the focus during the scans. The frontiers of the ROIs should approximately coincide with some visible frontiers of the different DUT blocks.
- The test sequence and scan mode can be adjusted for each ROI in order to optimize the detection of specific events and the beam time.
- When possible, the threshold for SEU of a single-bit in a memory structure (embedded SRAM, registers) should be accurately determined first to estimate the useful energy range.
- The DUT may exhibit a significant number of SEFIs with different and rare signatures related to unique resources and short vulnerability windows.
- Laser-triggered high current events that are not SELs may be observed as a consequence of a bus contention or other architecture related effects.

13. Limitations and undesirable effects

13.1. Lack of dielectric ionization

Ionizing particles from radiation environments have enough energy to create electron-hole pairs in any material that constitutes the active stack of a component, including the dielectric layers. Ionization of the gate dielectric is assumed to be at the origin of, or to contribute to, certain types of SEEs like SEGR in power MOSFETs and SEUs in flash memory cells.

The energy of the photons used for SEE laser testing of silicon devices, in the near-infrared part of the spectrum, can only create pairs in the semiconductor layers. In SiO_2 or other dielectric layers, those photons may only ionize shallow traps. Creating pairs in dielectrics requires photons in the UV range, which are absorbed in such short distances in silicon that they are of limited practical interest for laser SEE testing.

This implies that SEE laser testing facilities should not be used in an attempt to reproduce SEEs in which the ionization of a dielectric layer is at least partially involved.

Guideline #29

Laser testing in its common form is not appropriate for testing for single-events that require ionization of a dielectric layer.

13.2. Spot size effects

The initial radial profile of laser-induced and particle-induced charge tracks have different widths. The radial profile of an ion track strongly depends on the energy of the particle, but the order of magnitude of its characteristic diameter is usually considered to be in the sub-100nm range, although some of the high energy primary electrons (delta-rays) generated may reach much larger distances from the track center. For a laser-induced track, the order of magnitude is in the 1µm range. This factor 10 difference in the scale of the initial charge distribution may lead to differences in the initial response of the elementary structures, which could contribute to differences in the threshold amount of charge that has to be generated to produce an event and thus, in threshold-based correlation between laser and heavy ion measurements. Note that, due to carriers diffusion, the difference in the radial profiles tends to diminish in the first tens of picosecond after the interaction, and is of limited practical significance in the majority of SEE studies, although there are cases where this difference is significant.

The larger size of the laser-induced charge track can also lead to an overestimation of the cross section. The magnitude of this overestimation depends on the fragmentation of the sensitive area of the DUT, so it tends to be higher at low energies. Methods have been proposed to account for this effect in specific cases [28, 29].

13.3. Reflections on metal layers

In the backside testing approach, a fraction of the beam that is not absorbed in silicon can be reflected by metal contacts and metal interconnexion lines back into the semiconductor. This phenomenon may increase the amount of charge generated in the semiconductor. This has been experimentally observed with TPA on test structures [30]. The phenomenon is expected to be more present with SPA. Indeed, SPA is more tolerant than TPA to wave-front distortions introduced by diffraction and reflections on an irregular surface composed of thin metal lines and sub-wavelength sized metal contacts. Due to diffraction, the contribution of reflection is expected to be more important where the first metal layer structures are larger than the laser spot size, which is more probable in linear and power devices than in deep sub-micron technologies.

In practice, it is impossible to estimate the contribution of reflection at any location in a device without an accurate construction analysis and the topology details, which are, in most cases, not available. A rough upper limit can be estimated by considering that 100% of the beam would be reflected into the silicon. The resulting uncertainty on the effective amount of injected charge can be considered when processing and reporting the results by including an asymmetrical (positive only) error bar on the laser pulse energy.

Note that, since reflections tend to increase the amount of charge generated, neglecting those reflections when estimating the amount of charge deposited by a laser pulse is a conservative approach in terms of SEE sensitivity estimation, as it would lead to an under-evaluation of the threshold energy to trigger an event.

13.4. Reflection and transmission by buried oxide in SOI technologies

The buried oxide (BOX) layer in SOI technologies acts as a Fabry-Perot etalon, the transmission of which can vary significantly with the thickness of the BOX. As an example, figure 13.1 presents the transmittance of a BOX as a function of the BOX thickness with a lightly doped Si substrate and a thick film. Considering that the BOX is located near the beam-waist where the beam can be approximated to a plane wave, the transmittance can be estimated using a thin-film matrix approach [5].

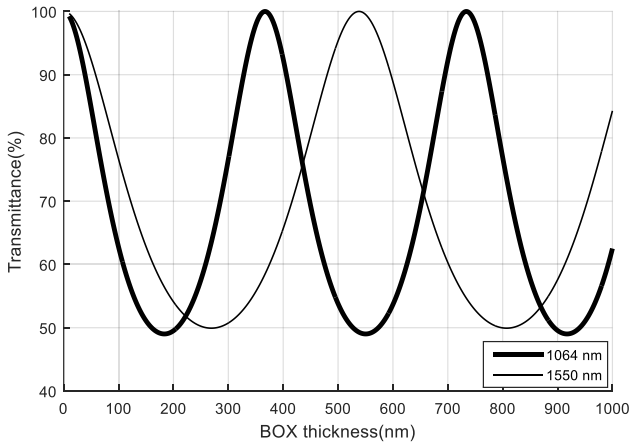

Fig. 13.1: buried oxide (BOX) transmittance as a function of its thickness, considering a lightly doped Si

13.5. Laser-induced degradation

At sufficiently high pulse energy or high average power, a laser beam can induce permanent degradations in the DUT through different mechanisms that are not related to SEEs.

The first macro-mechanism to consider is local thermally induced degradation related to an excessive average power of the beam. When the heat accumulation from pulse to pulse is higher than the ability of the structure to dissipate the heat, the average temperature in the laser spot region will increase. Maintaining this local temperature above a certain threshold for a sufficient amount of time can activate different transformations of the device physical properties that can result in a degradation of its electrical characteristics and a loss of functionality. The possible degradation micro-mechanisms are numerous and depend on the DUT technology. Since the average power of the beam is the product of the laser pulse energy with the pulse frequency, a simple precaution to prevent heat accumulation is to keep the pulse frequency as low as possible.

With very low pulse frequency or in single-shot mode, degradation may also be induced by a single pulse of sufficiently high energy [32]. Such degradation will accumulate if several pulses are delivered to the same spot [33, 34].

14. Elements for SPA equivalent LET estimation

14.1. Relationship between laser-induced charge and SEE occurrence

The possibility of theoretically defining an equivalence between a laser pulse energy and an LET relies on the definition of a criterion for establishing this correspondence. A classical criterion commonly used in the field of radiation effects is the critical charge deposited in a sensitive volume, which provides a simple relationship between the generated charge and the occurrence of an SEE. This simple model of the charge-SEE relationship has well-known limitations, including the difficult definition of a sensitive volume, which is assumed to incorporate all the complexity of the various charge collection mechanisms and hide it behind a few geometrical parameters and a critical charge criterion. Despite its limitations, this approach has been extensively used and has proven to be useful for SEE analysis and rate prediction, and this is the basis that is also commonly used for calculating the equivalent LET of a laser pulse and that is used hereafter. The critical charge criterion allows for a calculation-based approach of the laser/ion equivalence. Note that other criteria are possible that may be used for an experimental calibration-based approach of the equivalence like, for example, the amplitude of a particular SET.

14.2. Equivalent LET estimation

With the limitations of the RPP and critical charge model, the calculation method presented below should be considered as a first-order approach to estimate the order of magnitude of the equivalent LET of a laser pulse, or to estimate the laser pulse energy range of interest for an experiment.

14.2.1. Principles

Considering an ion of LET L impinging at normal incidence in a sensitive volume of thickness d_V, the charge generated in the sensitive volume is given by:

$$Q = \frac{L\, d_V}{E_p}\, q \tag{14-1}$$

where E_p is the average ionization energy (3.6 eV in Si) and q is the elementary charge.

For a laser pulse, the amount of charge generated in the same volume can be calculated by integrating the laser-induced generation rate:

$$Q = q \iiint_V \int_{-\infty}^{+\infty} G(\boldsymbol{r}, t) dt\, d\boldsymbol{r} \tag{14-2}$$

Note that the range of the time integral assumes that the pulse duration is short enough for considering the charge generation as instantaneous with respect to the device's reaction time.

Assuming that an ion and a laser pulse are equivalent when they deposit the same amount of charge in the sensitive volume V, the equivalent LET of a laser pulse is obtained by equalizing (14-1) and (14-2):

$$L = \frac{E_p}{d_V} \iiint_V N(\boldsymbol{r}) \tag{14-3}$$

where $N(r)$ is the laser-induced charge distribution, i.e. the integral over time of the charge generation rate. (14-3) can be used for both SPA and TPA with the appropriate numerical modelling of the laser-induced charge distribution [31]. Closed-form approximations can also be derived in specific cases with additional approximations.

For SPA backside testing at 1064nm with pulse duration >10ps and pulse energies below a few nJ, a first approximation of the equivalent LET is given by:

$$L = K_{SPA}E \tag{14-4}$$

where *E* is the incident laser pulse energy. Assuming that the thickness of the sensitive volume is small compared to the penetration depth of the beam, the proportionality coefficient is then given by:

$$K_{SPA} = \alpha_{IB}T_b e^{-\alpha d_s}T_{box}\frac{E_p}{E_\gamma} \tag{14-5}$$

where T_b is the transmission coefficient of the backside surface, d_s is the substrate thickness, E_γ is the photon energy, T_{box} is the total transmission of the buried oxide layer for SOI devices and equals to 1 for bulk devices, and α_{IB} and α are the band-to-band and total absorption coefficients, respectively, as defined in section 3.1.

14.2.2. Possible additional considerations

Depending on the DUT technology and test conditions, a careful expertise can be required to adapt the model above in order to include additional correction factors. A few examples of model improvements are listed below.

Equation (14-3) is based on the time integration of the laser-induced charge generation rate over the entire pulse duration. When the device's reaction time is known to be of the same order of magnitude as the laser pulse duration, the device's reaction time should be used as the positive limit of time integration. This correction tends to reduce the equivalent LET of a given laser pulse energy.

Equations (14-4) and (14-5) are based on the integration of the laser-induced charge distribution over the infinite radial plane, which neglects the effect of laser spot size. In recent technologies, it may be necessary to define a sensitive volume of finite radial extent with dimensions related to the elementary transistor topology. This correction tends to reduce the equivalent LET of a given laser pulse energy.

Equations (14-5) neglects the attenuation of the laser beam within the sensitive volume. With SPA at 1064nm, this should only be corrected when dealing with sensitive volumes thicker than 10µm.

While equations (14-1) and (14-2) assumes a single sensitive volume with uniform charge collection efficiency, they can be easily extended to the case where a distribution of sensitive volumes having different collection efficiencies provides a better representation of the SEE mechanism.

15. Guidelines recapitulation

16. References

[1] ESCC 25100, Single Event Effects Test Method and Guidelines

[2] JEDEC JESD57A, Test Procedures for the Measurement of Single Event Effects in Semiconductor Devices from Heavy Ion Irradiation

[3] A.E. Siegman, *Lasers*, University Science Books, Mill Valley, California, 1986.

[4] A.E. Siegman, S. Townsend, « Output Beam Propagation and Beam Quality from a Multimode Stable-Cavity Laser », IEEE J. Quantum Electron., 29, p. 1212, 1993.

[5] H. A. Macleod, “Thin-Film Optical Filters”, 2nd Edn, Adam Hilger Ltd., Bristol, 1986

[6] J.I. Pankove, *Optical processes in semiconductors*, Dover pub. New York, 1971.

[7] H.A. Weakliem, D. Redfield, “Temperature dependence of the optical properties of silicon”, J. Appl. Phys, vol 50, p. 1491, 1979.

[8] G. E. Jellison, F. A. Modine, “Optical absorption of silicon between 1.6 and 4.7 eV at elevated temperatures”, Appl. Phys. Lett., vol 41, p 180, 1982.

[9] R. Loudon, *The quantum theory of light*, Clarendon Press, Oxford, 1972.

[10] P.E. Schmid, “Optical absorption in heavily doped silicon”, Phys. Rev. B, vol 23-10, 1981.

[11] R.W. Boyd, *Nonlinear Optics*, second edition, Academic Press, London, 2003.

[12] R. Soref and B. Bennett, "Electrooptical effects in silicon," *Quantum Electronics, IEEE Journal of*, vol. 23, pp. 123-129, 1987.

[13] S. Buchner, F. Miller, V. Pouget, D. McMorrow, “Pulsed-Laser Testing for Single-Event Effects Investigations”, IEEE Trans. Nucl. Sci., vol 60-3, p. 1852, 2013.

[14] C. Xu, W. Denk, “Two-photon optical beam induced current imaging through the backside of integrated circuits”, Appl. Phys. Lett., 71 (18), p. 2578, 1997.

[15] McMorrow D., Lotshaw W.T., Melinger J.S., Buchner S., Boulghassoul Y., Massengill L.W., and Pease R., "Three dimensional mapping of single-event effects using two-photon absorption", IEEE Trans. Nuc. Sci., vol. 50, pp. 2199-2207, 2003.

[16] D. Lewis, V. Pouget, F. Beaudoin, P. Perdu, H. Lapuyade, P. Fouillat, A. Touboul, “Backside laser testing for SET sensitivity evaluation”, IEEE Trans. Nucl. Sci., 48, p 2193, 2001.

[17] K. Shao, V. Pouget, E. Faraud, C. Larue, D. Lewis, “Comparison of classical and two-photon photoelectric laser stimulation capabilities for failure analysis”, Proc. of IPFA 2011

[18] E. Faraud, V. Pouget, K. Shao, C. Larue, F. Darracq, D. Lewis, A. Samaras, F. Bezerra, E. Lorfevre, R. Ecoffet, “Investigation on the SEL Sensitive Depth of an SRAM Using Linear and Two-Photon Absorption Laser Testing”, IEEE Trans. Nucl. Sci., vol 58-6, p. 2637, 2011.

[19] F. Darracq, N. Mbaye, S. Azzopardi, V. Pouget, E. Lorfevre, F. Bezerra, D. Lewis, “Investigation on the Single Event Burnout Sensitive Volume Using Two-Photon Absorption Laser Testing”, IEEE Trans. Nucl. Sci., vol 59-4 p. 999, 2012.

[20] V. Pouget, D. Lewis, and P. Fouillat, "Time-resolved scanning of integrated circuits with a pulsed laser: application to transient fault injection in an ADC," Instrumentation and Measurement, IEEE Transactions on, vol. 53, no. 4, pp. 1227-1231, 2004.

[21] A. Diaspro, Confocal and two-photon microscopy, Wiley-Liss, New-York, 2002.

[22] A. Douin, V. Pouget, F. Darracq, D. Lewis, P. Fouillat, P. Perdu, “Influence of Laser Pulse Duration in Single Event Upset Testing”, IEEE Trans Nucl Sci, vol 53, 4., pp. 1799-1805, 2006.

[23] H. H. Li, "Refractive index of silicon and germanium and its wavelength and temperature derivatives", Journal of Physical and Chemical Reference Data 9, 561-658, 1980.

[24] B. J. Frey, D. B. Leviton, T. J. Madison, "Temperature-dependent refractive index of silicon and germanium," Proc. SPIE 6273, Optomechanical Technologies for Astronomy, 62732J, 2006.

[25] M. A. Green, “Self-consistent optical parameters of intrinsic silicon at 300K including temperature coefficients”, Solar Energy Materials and Solar Cells, vol 92-11, pp. 1305-1310, 2008.

[26] K. G. Svantesson, N. G. Nilsson, “Determination of the temperature dependence of the free carrier and interband absorption in silicon at 1.06µm”, J. Phys. C: Solid State Phys., 12, 3837, 1979.

[27] F. Miller, S. Morand, A. Douin, R. Gaillard, T. Carrière, N. Buard, “Laser Validation of a Non-Destructive Test Methodology for the Radiation Sensitivity Assessment of Power Devices”, IEEE Trans. Nucl. Sci., vol. 58-3, p. 813, 2011.

[28] V. Pouget, P. Fouillat, D. Lewis, H. Lapuyade, F. Darracq, A. Touboul, “Laser cross section measurement for the evaluation of single-event effects in integrated circuits”, Microelectronics Reliability, vol. 40, October, 2000.

[29] F. Miller, N. Buard, T. Carriere, R. Dufayel, R. Gaillard, P. Poirot, J.- M. Palau, B. Sagnes, and P. Fouillat, “Effects of beam spot size on the correlation between laser and heavy ion SEU testing,” IEEE Trans. Nucl.Sci., vol. 51, no. 6, pp. 3708–3715, Dec. 2004.

[30] A. Khachatrian, N. Roche, N. Dodds, D. McMorrow, J. Warner, S. Buchner, R. Reed, "The Impact of Metal Line Reflections on Through-Wafer TPA SEE Testing," IEEE Trans. on Nucl. Sci., vol. 62, no. 6, pp. 2452-2457, 2015.

[31] V. Pouget, H. Lapuyade, P. Fouillat, D. Lewis, S. Buchner, “Theoretical Investigation on an Equivalent Laser LET”, Microelectronics Reliability, 41, p 1513, 2001

[32] D. Perez, L. Lewis, “Ablation of Solids under Femtosecond Laser Pulses”, Phys. Rev. Let., vol 89-25, 2002.

[33] O. Armbruster, A. Naghilou, M. Kitzler, W. Kautek, “Spot size and pulse number dependence of femtosecond laser ablation thresholds of silicon and stainless steel”, Applied Surface Science, vol 396, pp. 1736-1740, 2017.

[34] M.E. Shaheen, J.E. Gagnon, B.J. Fryer, “Studies on laser ablation of silicon using near IR picosecond and deep UV nanosecond lasers”, Optics and Lasers in Engineering, vol 119, pp 18-25, 2019.

[35] A. Balasubramanian et al., "Pulsed Laser Single-Event Effects in Highly Scaled CMOS Technologies in the Presence of Dense Metal Coverage," in IEEE Trans. Nucl. Sci., vol. 55, no. 6, pp. 3401-3406, 2008

17. APPENDIX 1 – Sample test-sheet for SEE laser testing

The table below presents the typical structure of a test sheet that should be completed during a laser testing campaign. The structure may be adapted to the specific design of the experiment.

SESSION

Campaign ID:
Facility ID:

Facility parameters:
Wavelength:
Pulse duration:
Lenses:

ID	NA

Room temperature:

Notes:

Device under test:
Reference:
Technology:
Die dimensions:
Test approach (front-side/backside):
Samples:

ID	Substrate thickness	Observation

Test bench description:

RUNS

Run information						Testbench parameters						Scan parameters												Beam parameters			Observations
												Region of interest										Scan mode	Lens ID				
						Parameter 1		Parameter 2		Parameter 3		Name	Coordinates						Steps								
Run ID	Goal	Date	Time	Duration	DUT Sample ID	Name	Value	Name	Value	Name	Value		Xmin	Xmax	Ymin	Ymax	Zmin	Zmax	dX	dY	dZ			Pulse Energy	Pulse Frequency	Delivered pulses count	